# STUDY OF LITHIUM SOLVATION ENVIRONMENTS IN WATER-SATURATED NITROBENZENE

A Thesis
Presented to
The Academic Faculty

by

Greg Moakes

In Partial Fulfillment
of the Requirements for the Degree
Doctor of Philosophy in the
School of Chemistry and Biochemistry

Georgia Institute of Technology
December 2006

# STUDY OF LITHIUM SOLVATION ENVIRONMENTS IN WATER-SATURATED NITROBENZENE

Approved by:


Dr. Jiří Janata, Advisor
School of Chemistry and Biochemistry
*Georgia Institute of Technology*

Dr. Leslie T. Gelbaum
School of Chemistry and Biochemistry
*Georgia Institute of Technology*

Dr. Lawrence A. Bottomley
School of Chemistry and Biochemistry
*Georgia Institute of Technology*

Dr. L. Andrew Lyon
School of Chemistry and Biochemistry
*Georgia Institute of Technology*

Dr. Charles A. Eckert
School of Chemical and Biomolecular Engineering
*Georgia Institute of Technology*


Date Approved: November 7, 2006

To Mum and Dad

# ACKNOWLEDGEMENTS

It is a great honor to express my sincerest thanks to my advisor, Professor Jiří Janata, and Dr. Mira Josowicz for their endless support and guidance throughout my graduate studies. I would also like to thank Dr Lawrence Bottomley, Dr Charles Eckert, Dr Leslie Gelbaum and Dr Andrew Lyon for serving on my thesis advisory committee. I am extremely grateful to Dr Johannes Leisen and Dr Vladimir Marecek for their constant support and offering of expertise throughout my project.

I would like to thank my group members for their friendship, assistance and unfailing ability to contribute to interesting discussion.

I would like to thank my family for their eternal support in matters of both research and my pursuit of personal happiness. I would also like to give thanks to my American family, Lyndsay, Martha and Michael Fry, whose selflessness and support has made life in a different country immensely pleasurable.

# TABLE OF CONTENTS

# LIST OF TABLES

# LIST OF FIGURES

# SUMMARY

The field of study on processes occurring at the liquid-liquid interface is discussed in chapter 1. A general introduction to the importance of study and the previous experimental methods is covered along with an introduction on how molecular spectroscopy can be used to study the kinetics and mechanism of transfer for species at the liquid-liquid interface. Chapter 2 describes the use of $^{7}$Li NMR for study of 'solvatomers' of Lithium in water-saturated nitrobenzene. The study of lithium salts of varying hydrophobicity has revealed the presence of multiple metastable solvation states of lithium in a mixed water/nitrobenzene system. The kinetics of exchange between these solvation states has also been studied and is reported in this chapter.

In chapter 3, the use of $^{7}$Li NMR for solvation studies is supplemented with $^{2}$H NMR. The use of deuterium NMR allows the consideration of solvation states from the point of view of the aqueous phase rather than the solvated species, lithium. The occurrence of the metastable solvation states can also be seen by $^{2}$H NMR but more interestingly, the high concentration of water in the samples compared to lithium allows diffusion-ordered spectroscopy study of the system. This leads to calculation of the diffusion coefficient of these solvation states. It is reported that addition of lithium salts, while clearly affecting the nature of hydrogen bonding, does not significantly influence the size of hydrated species. In chapter 4, the mixed water/nitrobenzene system is studied by FTIR. The OH stretch of water is affected greatly by the degree of hydrogen bonding. This allows study of the affect of lithium salts on the degree of hydrogen bonding in

water-saturated nitrobenzene. The downside of the FTIR study is that only OH stretches resulting from 'free OH' are visible. This is because the IR stretch of the majority solvent, nitrobenzene, obscures stretches resulting from hydrogen-bonded water. This can be overcome by conducting inelastic neutron scattering studies on the system, as discussed in chapter 5. The difference in inelastic neutron scattering coefficient between hydrogen and dueterium allows subtraction of the scattering pattern for nitrobenzene. The hydrogen-bonding character of water can therefore be elucidated from the neutron scattering pattern of $H_2O$ in deuterated nitrobenzene. Since deuterium gives near-zero neutron scattering, the scattering pattern gives information about the state of water in nitrobenzene. Chapter 6 details the use of Laser Induced Breakdown Spectroscopy (LIBS) to asses the extent of ion incorporation in glass during the solvation study experiments. The increased activity of the lithium ion in a majority organic medium appears to drive the ion to the hydrated layer on the glass surface. The use of this technique for low energy, low-cost doping of glass is discussed. Chapter 7 is a discussion of overall conclusions and Chapter 8 is a look towards future work.

# CHAPTER I

# INTRODUCTION

## 1.1 Liquid-liquid Interface

The study of the interface between two immiscible liquids is of theoretical and practical interest. The results of liquid-liquid interface studies can impact many other fields of study. For example, in biochemistry, an understanding of interfacial structure, kinetics and thermodynamics is critical for biological membrane modeling.[1] In electrochemistry, liquid-liquid interface studies have been used in sensor design[1-3] and to understand processes occurring in ion-selective electrodes with liquid membranes.[1,4] Analysis of processes taking place during phase transfer catalysis (PTC) also requires an understanding of interfacial chemistry.

The interface between two immiscible electrolyte solutions (ITIES) is formed between two solvents of low miscibility,[1] each containing an electrolyte. Typically, one of these solvents is water and the other is a polar organic solvent with a moderate to high dielectric permittivity.[1] The most common second solvent is nitrobenzene. Both electrochemical[5-11] and spectroscopic[12-15] techniques have been used in the study of ITIES. The questions of interest involve both thermodynamics and kinetics of ion transfer between the two phases. The role of water in the ion transfer has been the focus of work of several groups. Among these studies the work of Osakai's group occupies the most prominent role.[16-20] The work of Osakai et. al has focused on the affect of temperature

and dissolved electrolyte on the $^{1}H$ chemical shift of water dissolved in an organic solvent.[16-20]

Of primary interest for study is the determination of the Gibbs free energy of transfer for species across the liquid-liquid interface and elucidation of the mechanism by which the species transfers.[15,16,20] A solid understanding of ion transport mechanisms across the interface of two immiscible liquids is fundamental to understanding electrochemistry[21-23] and surfactant chemistry.[24-26] It is also closely related to environmental problems such as separations chemistry that is performed in binary solvent systems (i.e., organic and aqueous phases) and interactions of contaminated organic solvents with ground water. Understanding ion transfer at the liquid-liquid interface is also critical to the study of the movement of species at biological interfaces.[27-29] Application of ITIES studies to the movement of pharmaceutical agents across the blood brain barrier is critical to understanding the pharmacokinetics in drug design.[27-29] Nitrobenzene/water is the most widely studied and understood interface between two immiscible electrolytes (ITIES)[1]

## 1.2 Electrochemistry at the liquid-liquid interface

The primary mode of study for ion transfer across the liquid-liquid interface has been by electrochemical methods.[5-11] The idea is to provide an ion with the Gibbs energy of transfer it requires to traverse the liquid-liquid interface.[16] This is achieved by polarizing the interface so that the Galvani potential difference,

$$\Delta_O^W \phi = \phi^W - \phi^O ,$$

where $\phi$ is the inner (Galvani) potential of the phase, compensates the Gibbs energy of transfer. The subscripts W and O represent the water and organic phase, respectively. At equilibrium, the equality of electrochemical potentials of ions in the two phases leads to the Nernst equation for ion transfer reactions:

$$\Delta_O^W \phi = \Delta_O^W \phi_i^o + RT / z_i F \ln(a_i^O / a_i^W) \quad [30]$$

Where F is the Faraday constant, $a_i$ and $z_i$ are the activity and charge of the ion i and $\Delta_O^W \phi_i^o$ is the standard transfer potential defined as:

$$\Delta_O^W \phi_i^o = \Delta G_{tr,i}^{o,W/O} / z_i F \quad [30]$$

Where $\Delta G_{tr,i}^{o,W/O}$ is the standard Gibbs energy of transfer for an ion from the water to the organic phase.

Both galvanostatic and potentiostatic methods have been used to study polarization of the liquid-liquid interface. Methods such as current-step chronopotentiometry[31] and chronocoulometry[32], potential step chronoamperometry[33], cyclic[34] and convolution voltammetry[35], ac voltammetry[36] and equilibrium impedance[37]

measurements have led to insights into kinetic information and Gibbs free energy of ion transfer. However, much is still debated. For example, Osakai et al argue that the evaluation of Gibbs free energy of ion transfer at ITIES works on the false assumption of a Born-type electrostatic solvation model.[20] In this model, the ion is considered as a hard sphere of radius r that is immersed in a continuous medium of constant permittivity. The transfer energy is calculated as a difference between electrostatic energies for charging the ion up to ze (e is the elementary charge) in organic, O and water, w phases:

$$\Delta G^{o}_{tr,i}{}^{w/o}(\text{Born}) = - N_A z^2 e^2 / 8 \pi \varepsilon_o r (1 / \varepsilon^o - 1 / \varepsilon^w) \quad [20]$$

Where $N_A$ is the Avagadro constant, $\varepsilon_o$ is the permittivity of vacuum and $\varepsilon^o$ and $\varepsilon^w$ are relative permittivities of O and W, respectively. Osakai's work realized that since organic solvents can dissolve significant amounts of water (200 mM for nitrobenzene) ions likely cross the liquid-liquid interface in hydrated form, as illustrated in figure 1.1. Realising this assumption and subsequently modifying the Born model so that it takes into account the hydration numbers and subsequent hydrodynamic radii of ions leads to closer agreement between models and experimental data.[20] While the consideration of ions as hydrated species has lead to greater understanding of the thermodynamics of ion transfer, the kinetics and mechanisms of transfer are still not largely understood. Ions transferring across this interface must exchange their solvation shell or maintain it in some metastable arrangement with their new environment. It stands to reason that the solvation exchange processes are not infinitely fast, in fact some of them may be unexpectedly slow, leading to the existence of metastable solvation states of the exchanging ion. The number of these

different solvatomers and their structures are not known, but a general schematic of the possible species involved in ITIES is proposed in figure 1.2. The details of the solvation mechanism depend on the location at which the solvation/resolvation process takes place,[18-20] on the concentration of the ions and on the local activity of water. That, in turn, depends on the structure of the L/L interface.

As stated, the majority of work on ion-transfer at the liquid-liquid interface has been performed using electrochemical techniques. This comes with a major drawback. The Galvani potential of a phase is established as soon as the ion of interest crosses the interface[1], irrespective of the form this species takes i.e. its solvation environment. It is because of this fact that electrochemistry alone cannot elucidate solvation processes and structure of species in solution.

The aim of this work has been to use non-invasive spectroscopic techniques to assess the dynamic processes occurring when an ion transfers across the liquid-liquid interface. Also of interest are the resulting solvation environments of ions after transferring from the water to organic phase.

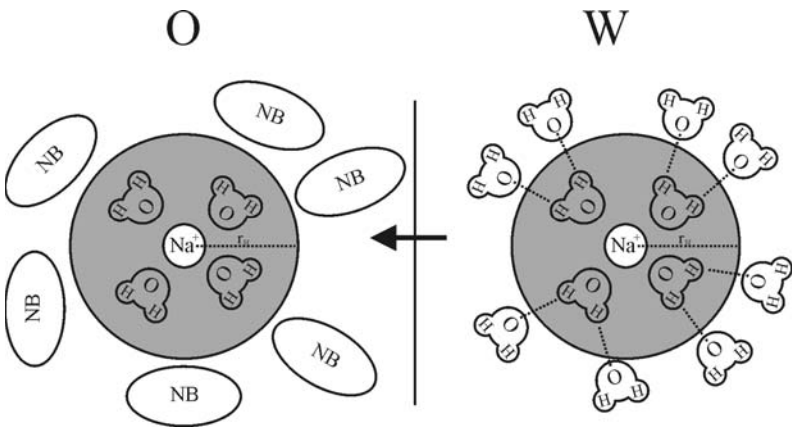


Figure 1.1: When an ion transfers from the aqueous to organic phase, its hydration number and hydrodynamic radii will likely influence the solvation environment in the organic phase.

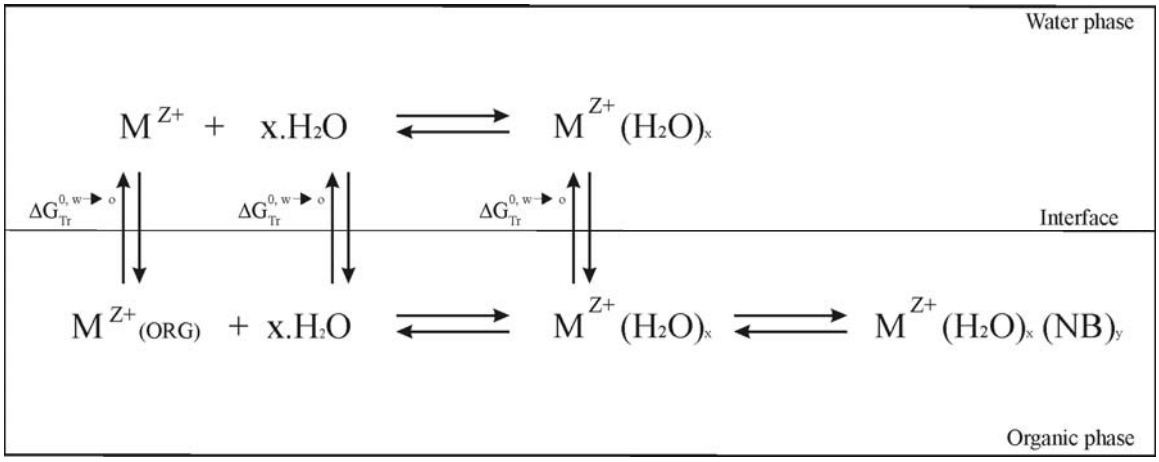


Figure 1.2: Illustration of the potential ion transfer situations at the liquid-liquid interface depending on hydrophobicity of ion.

# CHAPTER II

# $^{7}$Li NMR STUDY OF LITHIUM SALTS IN WATER-SATURATED NITROBENZENE

## 2.1 Introduction

The major drawback of studying ion transfer at the liquid-liquid interface by electrochemical methods is that the system must be perturbed in order to gain information such as the Gibbs free energy of transfer.[1] There has been recent interest in the use of spectroscopic techniques to elucidate kinetics and mechanisms of ion transfer.[16-20] Proton NMR spectroscopy has been a standard technique of study of solvation in homogeneous phases[16] and at interfaces.[38] Electrochemical *in situ* experiments at solid electrodes have been investigated by solid phase NMR as a new powerful auxiliary technique.[39] While much work has been undertaken to probe the thermodynamics of ion transfer at ITIES, the identities of solvatomers that an exchanged ion forms in nitrobenzene, the most common second solvent, are still not fully understood. Factors affecting the degree of hydration of ions in organic solvents have been studied by many methods, including FTIR and NMR.[16-18, 40] The hydration numbers of different anions in nitrobenzene and their effect on $^{1}$H chemical shifts has been studied by $^{1}$H NMR.[19] Proton NMR has also been used to explain how the water content of nitrobenzene affects the hydration of ions in the solvent.[16] However, the abundance of hydrogen atoms on nitrobenzene makes $^{1}$H NMR study of solvation in nitrobenzene difficult. Detailed in this chapter is the use of $^{7}$Li NMR to investigate the dynamics and the effect of anion identity and water content on

the formation and decay of metastable solvatomers of $Li^+$ in the $Li^+$/nitrobenzene/water system. By using $Li^+$ as the NMR active nucleus, solvation effects can be directly observed as changes in the number of $^7Li$ resonances and their corresponding chemical shifts, with no interference from the protons of water or nitrobenzene. The important questions this work sought to answer are: what is the solvation environment of ions that have traversed across the water/organic interface into nitrobenzene? Are the solvation environments stable or dynamically changing? Finally how does the identity of the ion affect its solvation environment? To assess the effect of ion identity on solvation environment in nitrobenzene, data on hydrodynamic radii and Gibbs free energy of transfer was gathered[20] (tables 1 and 2) and salts were chosen for investigation that would represent a range of hydrophobicity. Since the first mode of investigation was $^7Li$ NMR, The cation used was $Li^+$ throughout all experiments. The lithium cation has hydrodynamic radius, $r_h$ = 0.351 nm and Gibbs free energy of transfer, $\Delta G_{tr}^{O/W}$ = -38.2 $KJmol^{-1}$.[20] The three salts chosen were lithium bromide (LiBr), lithium perchlorate ($LiClO_4$) and lithium undecamethyl carba-closo-dodecaborate ($LiHCB_{11}Me$). The bromide anion has hydrodynamic radius, $r_h$ = 0.276 nm and Gibbs free energy of transfer $\Delta G_{tr}^{O/W}$ = -27.8 $KJmol^{-1}$. The perchlorate cation has crystallographic radius, $r_h$ = 0.236 nm but a zero hydration number, leading to an incalculable hydrodynamic radius. The perchlorate anion has Gibbs free energy of transfer $\Delta G_{tr}^{O/W}$ = -7.9 $KJmol^{-1}$. The undecamethyl carba-closo-dodecaborate anion was developed in the laboratory of Dr Josef Michl specifically for its immense hydrophobicity. No data is available for this anion but it has close to zero solubility in water and thus is assumed, converse to the

other two anions, to have a positive Gibbs free energy of transfer from nitrobenzene to water.

An unexpected result is the effect of the wall of the vessel on the decomposition kinetics of the metastable solvatomers. It has been found that the solvation equilibria are dominated by slow kinetics involving mixed solvatomer $Li_{(nitrobenzene/water)}$.

Table 1.1: Charge numbers and Radii of ions, their hydration numbers and hydrated radii in nitrobenzene at 25 º C. [20]

Terms: z is the charge of the ion, $r^a$ is the crystallographic radius, $n^b$ is the number of moles of water coextracted into nitrobenzene per ion and $r_h^c$ is the resulting hydrodynamic radius.

| ion | $z$ | $r^a$ (nm) | $n^b$ | $r_h^c$ (nm) |
|---|---|---|---|---|
| (hydrated cations) | | | | |
| $Li^+$ | 1 | 0.073 | 6.0 | 0.351 |
| $Na^+$ | 1 | 0.116 | 3.8 | 0.307 |
| $K^+$ | 1 | 0.152 | 1.0 | 0.220 |
| $Rb^+$ | 1 | 0.166 | 0.7 | 0.212 |
| $Cs^+$ | 1 | 0.181 | 0.4 | 0.206 |
| $Ca^{2+}$ | 2 | 0.114 | 14 | 0.467 |
| $Ba^{2+}$ | 2 | 0.149 | 11 | 0.435 |
| (nonhydrated cations) | | | | |
| $Me_4N^+$ | 1 | 0.279[d] | 0 | |
| $Et_4N^+$ | 1 | 0.337[d] | 0 | |
| *n*-$Pr_4N^+$ | 1 | 0.379[d] | 0[k] | |
| *n*-$Bu_4N^+$ | 1 | 0.413[d] | 0 | |
| $Ph_4As^+$ | 1 | 0.426[e] | 0 | |
| $[Ni(bpy)_3]^{2+}$ | 2 | 0.527[f] | 0[k] | |
| $[Ni(phen)_3]^{2+}$ | 2 | 0.544[f] | 0[k] | |
| $[Fe(phen)_3]^{2+}$ | 2 | 0.541[f] | 0[k] (0.3) | |
| (hydrated anions) | | | | |
| $Cl^-$ | −1 | 0.167 | 4.0 | 0.322 |
| $Br^-$ | −1 | 0.182 | 2.1 | 0.276 |
| $I^-$ | −1 | 0.206 | 0.9 | 0.248 |
| $SCN^-$ | −1 | 0.213[g] | 1.1 | 0.260 |
| $NO_3^-$ | −1 | 0.189[h] | 1.7 | 0.267 |
| (nonhydrated anions) | | | | |
| $ClO_4^-$ | −1 | 0.236[h] | 0[k] (0.2) | |
| $IO_4^-$ | −1 | 0.249[h] | 0[k] | |
| 2,4-dinitrophenol$^-$ | −1 | 0.315[i] | 0[k] | |
| 2,4,6-trinitrophenol$^-$ | −1 | 0.332[i] | 0[k] | |
| $Ph_4B^-$ | −1 | 0.421[e] | 0 | |
| (polyanions) | | | | |
| α,β-$[XM_{12}O_{40}]^{4-}$ (X = Si, Ge; M = Mo, W) | −4 | 0.56[j] | 0[k] | |
| α,β-$[XM_{12}O_{40}]^{3-}$ (X = P, As; M = Mo, W) | −3 | 0.56[j] | 0[k] | |
| α-$[X_2Mo_{18}O_{62}]^{6-}$ (X = P, As) | −6 | 0.648[j] | 0[k] | |
| α-$[S_2Mo_{18}O_{62}]^{4-}$ | −4 | 0.648[j] | 0[k] | |
| $[S_2VMo_{17}O_{62}]^{5-}$ | −5 | 0.648[j] | 0[k] | |
| $[P_2Mo_{18}O_{61}]^{4-}$ (containing $P_2O_7^{4-}$) | −4 | 0.644[j] | 0[k] | |
| $[Mo_6O_{19}]^{2-}$ | −2 | 0.437[j] | 0[k] | |
| $[VMo_5O_{19}]^{3-}$ | −3 | 0.437[j] | 0[k] | |
| α-$[Mo_8O_{26}]^{4-}$ | −4 | 0.485[j] | 0[k] | |

Table 1.2: Standard Gibbs Energies of Transfer of Ions from NB to W and Their Charge-Independent and-Dependent Components at 25 °C[20]

| ion | $\Delta G_{tr}^{\circ,O\rightarrow W}$ (kJ mol$^{-1}$) | $\Delta G_{tr}^{\circ,O\rightarrow W}$ ($z$-indep)[a] (kJ mol$^{-1}$) | $\Delta G_{tr}^{\circ,O\rightarrow W}$ ($z$-dep)[b] (kJ mol$^{-1}$) |
|---|---|---|---|
| (hydrated cations) | | | |
| $Li^+$ | −38.2[c,o] | 23.6 | −61.8 |
| $Na^+$ | −34.2[c,o] | 17.9 | −52.1 |
| $K^+$ | −23.5[c,o] | 9.2 | −32.7 |
| $Rb^+$ | −19.4[c,o] | 8.6 | −28.0 |
| $Cs^+$ | −15.4[c,o] | 8.1 | −23.5 |
| $Ca^{2+}$ | −67.3[d,o] | 41.6 | −108.9 |
| $Ba^{2+}$ | −61.8[d,o] | 36.0 | −97.8 |
| (nonhydrated cations) | | | |
| $Me_4N^+$ | −3.4[c,o] | 14.8 | −18.2 |
| $Et_4N^+$ | 5.3[e] | 21.7 | −16.4 |
| $n$-$Pr_4N^+$ | 16.4[f] | 27.4 | −11.0 |
| $n$-$Bu_4N^+$ | 26.5[g] | 32.5 | −6.0 |
| $Ph_4As^+$ | 35.9[c,o] | 34.6 | 1.3 |
| $[Ni(bpy)_3]^{2+}$ | 30.5[h] | 53.0 | −22.5 |
| $[Ni(phen)_3]^{2+}$ | 41.3[h] | 56.4 | −15.1 |
| $[Fe(phen)_3]^{2+}$ | 44.0[i] | 55.8 | −11.8 |
| (hydrated anions) | | | |
| $Cl^-$ | −38.2[j] | 19.8 | −58.0 |
| $Br^-$ | −27.8[k] | 14.6 | −42.4 |
| $I^-$ | −18.4[k] | 11.7 | −30.1 |
| $SCN^-$ | −15.8[k] | 12.9 | −28.7 |
| $NO_3^-$ | −25.2[k] | 13.5 | −38.7 |
| (nonhydrated anions) | | | |
| $ClO_4^-$ | −7.9[k] | 10.6 | −18.5 |
| $IO_4^-$ | −6[l] | 11.8 | −17.8 |
| 2,4-dinitrophenol$^-$ | −5.7[m] | 18.9 | −24.6 |
| 2,4,6-trinitrophenol$^-$ | 6.7[m] | 21.0 | −14.3 |
| $Ph_4B^-$ | 35.9[c,o] | 33.8 | 2.1 |
| (polyanions) | | | |
| $\alpha,\beta$-$[XM_{12}O_{40}]^{4-}$ | 25.9[n] | 59.8 | −33.9 |
| $\alpha,\beta$-$[XM_{12}O_{40}]^{3-}$ | 71.8[n] | 59.8 | 12.0 |
| $\alpha$-$[X_2Mo_{18}O_{62}]^{6-}$ | 2.9[n] | 80.1 | −77.2 |
| $\alpha$-$[S_2Mo_{18}O_{62}]^{4-}$ | 103.8[n] | 80.1 | 23.7 |
| $[S_2VMo_{17}O_{62}]^{5-}$ | 41.0[n] | 80.1 | −39.1 |
| $[P_2Mo_{18}O_{61}]^{4-}$ | 92.2[n] | 79.1 | 13.1 |
| $[Mo_6O_{19}]^{2-}$ | 31.6[n] | 36.4 | −4.8 |
| $[VMo_5O_{19}]^{3-}$ | −34.4[n] | 36.4 | −70.8 |
| $\alpha$-$[Mo_8O_{26}]^{4-}$ | −52.9[n] | 44.9 | −97.8 |

## 2.2 Experimental

### 2.2.1 Materials

Lithium perchlorate and lithium bromide (≥ 99%, Aldrich) were used as received. Lithium undecamethyl carba-closo-dodecaborate was received from the research group of Professor Josef Michl at the University of Colorado, Denver, Colorado. Nitrobenzene (99%, ACROS Organics) was redistilled under vacuum and dried before use by molecular sieves (4A, Sigma–Aldrich). Glass 5mm NMR sample tubes were obtained from Wilmad-Labglass. All water used was de-ionized to 18 MΩ using a US-Filter Modulab water system (US Filter, Warrendale, PA). The Sephadex beads used in this work were purchased from Sigma–Aldrich (Milwaukee, WI) and the polystyrene beads were obtained from Duke Scientific, Corp. (Palo Alto, CA). The polystyrene–DVB beads (PS) were polydispersed 1–50 μm diameter, CAT # 445. The 25–100 μm, moderately hydrophobic lipophilic Sephadex beads (LS), CAT# LH 20 100 and the regular 100–300 μm hydrophilic Sephadex beads (HS) CAT# G 25 300 were used.

### 2.2.2 Procedures

Saturated solutions of LiBr, $LiClO_4$ and $LiHCB_{11}Me$ in dry NB were prepared by shaking excess of lithium salt with dry NB for 5 minutes and then allowing the mixture to equilibrate for 3 hrs prior to measurement. Saturated solutions of LiBr and $LiClO_4$ in water were prepared by adding LiBr, $LiClO_4$ to de-ionized $H_2O$ until solid salt remained.

For preparation of ‘‘wet’’ NB solution of LiBr, $LiClO_4$ and $LiHCB_{11}Me$, 5 mL of aqueous solution (saturated with salt of interest) was added to 20 mL of nitrobenzene. The two phase mixture was magnetically stirred for 24 h. When the stirring stopped the experimental clock was arbitrarily set to $t = 0$. The phases were allowed to separate for 3 h and after that 2–3 mL of the upper clear nitrobenzene phase were transferred into a clean vial and then to the NMR sample tube. The Lithium content of the "wet” NB solution was determined by atomic absorption spectroscopy to be $9.52 \times 10^{-4}$ M for Lithium Perchlorate and $1.43 \times 10^{-5}$ for Lithium Bromide. The published concentration of water in water-saturated ‘‘wet’’ nitrobenzene is between 170 and 190mM.[16]

The two phases were also used in the polymer bead experiments. The hydrophilic beads were first saturated with an aqueous solution of LiBr and then mixed with the LiBr-saturated nitrobenzene phase to form a thick paste. Similarly, nitrobenzene phase saturated with LiBr was confined to the lipophilic Sephadex or polystyrene beads, respectively. The aqueous phase saturated with LiBr was used to form a thick paste.

### 2.2.3 NMR experiments

The NMR spectra were recorded using a Bruker AMX-400 spectrometer (Bruker BioSpin, Rheinstetten, Germany) with a 5 mm and a 10 mm broadband probe. The $^7Li$ signal was observed at 155.5 MHz. with a 5 μs pulse ($30^0$) and a 2.3s pulse delay. A $^7Li$-NMR spectrum of saturated (6M) $LiClO_4$ in $H_2O$ was recorded before each experiment and the corresponding signal calibrated to 0 ppm. Kinetic data was recorded automatically using a macro. Typically, 30 successive experiments with a duration of 10 minutes separated by time delays of 15 min were measured. Peak areas were calculated

by a line fitting function of the Mestre-C NMR software **(**Mestrelab Research SL, Santiago de Compostela University, Santiago, Spain)**.** The line fit function uses the Levenberg-Marquardt non–linear least squares and Downhill Simplex (Nelder and Mead) algorithms for estimating peak parameters (position, intensity, line width and line shape function). Temperature of the NMR probe was controlled to an accuracy of ±1 K using the spectrometers VT accessories. No frequency lock was used in 5 mm probe. When the 10mm probe was used, Benzene-$d_6$ (99.96 atom.%d, Sigma–Aldrich), was sealed in a glass capillary which was inserted into the 10 mm sample tube as a field frequency lock. Since the acquisition of multiple spectra took several hours the experimental time for each set indicates the beginning of the NMR session. For sonication experiments the ultrasonic bath Aquasonic Model 150 HT, delivering an average sonic power of 135 W, was used.

## 2.3 Results

The $^{7}Li$ nucleus has a spin of 3/2 and a sensitivity which is 1540 times higher than $^{13}C$. NMR spectra of $^{7}Li^{+}$ in dry NB, water and ‘‘wet’’ NB are shown in figure 2.1. The chemical resonance of $^{7}Li$ in dry NB is shifted 1.280 ppm downfield, relative to the resonance in water. The $^{7}Li$ resonance peak in ‘‘wet’’ NB is significantly broader and lies between these two values.

### 2.3.1 NMR at the water–nitrobenzene interface

In order to obtain a sufficiently strong $^{7}$Li-NMR signal a high interface area has been realized by confining LiBr aqueous or NB phases in polymer beads (figure 2.2).

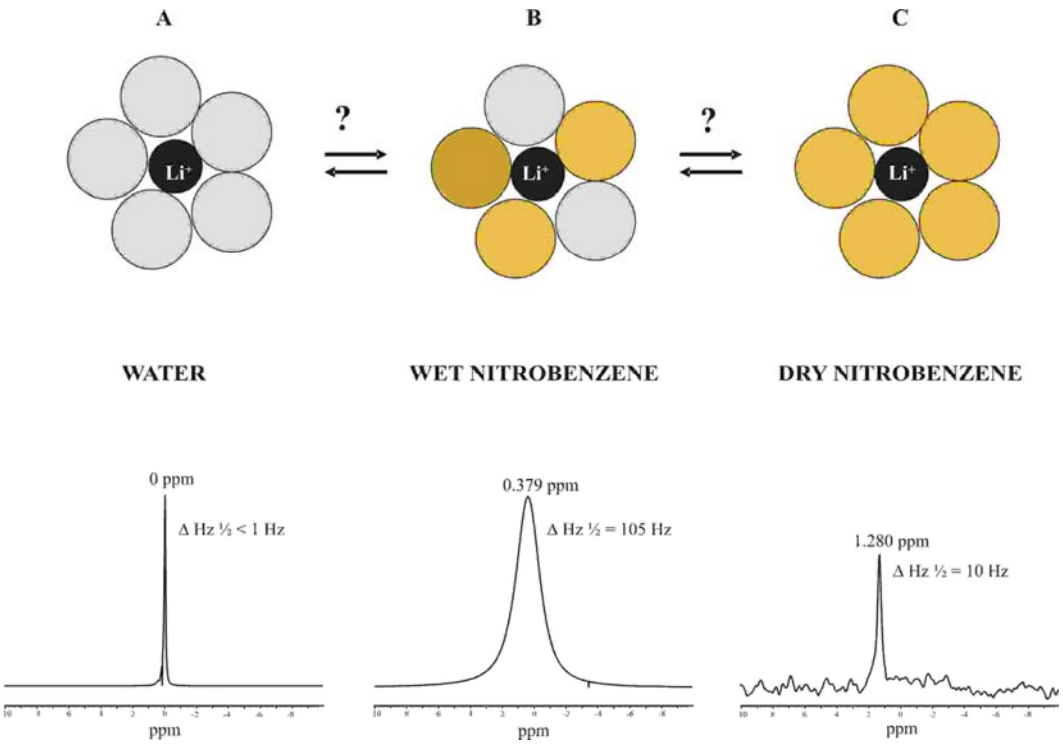


Figure 2.1: $^{7}$Li NMR resonance spectra of lithium ion solvated in three different environments and representation of the solvatomeric equilibria. (A) Water; (B) wet nitrobenzene; and (C) dry nitrobenzene.

The spectra of $^{7}$LiBr in dry NB and in water (Figure 2.1 A,C) show that it is possible to distinguish between the two distinctly different solvation environments of lithium, with a chemical shift separation of ~ 1.3 ppm. Hence, for the systems containing dispersed polymer beads and both solvents in intimate contact, one would expect spectra which are largely a superposition of spectra observed for Li dissolved in the aqueous phase (Figure 2.1 A) and Li dissolved in the wet nitrobenzene phase (Figure 2.1 C), especially if exchange behavior is fast.

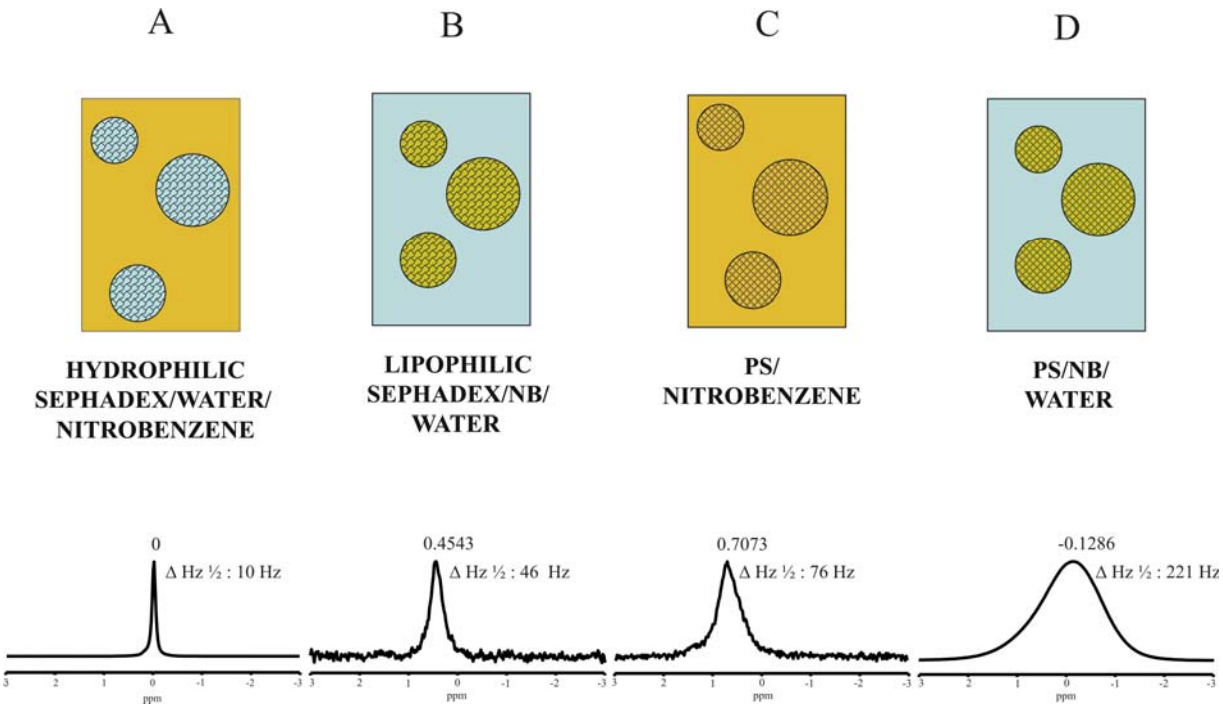


Figure 2.2: Realization of high interface area between nitrobenzene and water. One phase is confined in polydispersed polymeric beads which are then suspended in the other phase. Corresponding $^{7}$Li NMR spectra show different solvation states of the lithium ion.

Experimentally, for the system containing $LiBr_{(aq)}$/hydrophilic sephadex/bulk nitrobenzene, a narrow line was observed at 0 ppm, which is largely identical to the spectrum observed for LiBr dissolved in pure water. Hence, in this system the majority of Li ions will be dissolved in the water. For systems containing hydrophobic beads loaded with nitrobenzene, suspended in water, a rather broad peak is observed (Figure 2.2 B,D). For the most hydrophobic polymer beads (Figure 2.2 B, C, D) a peak is observed, which is broader than the one observed for Li ions dissolved in dry nitrobenzene (Figure 2.1 C). The rather broad peak may be viewed as $Li^+$ species experiencing different states of solvation. Each state of solvation will lead to a distinct chemical shift, however individual peaks, corresponding to different chemical solvation states are not resolved leading to a rather broad peak. In order to quantify the exchange rate between these species we have attempted to use 2D exchange spectroscopy (NOESY/EXSY). In this experiment, after the initial frequency labeling, the nuclei are given longitudinal Z magnetization with a second $90^\circ$ pulse. These vectors are now allowed to exchange through their dynamic process during the mixing time, leading to cross peaks in the 2D spectrum. The relative intensity of the off diagonal signal observed as a function of the mixing time allows the evaluation of the exchange rate. We chose to carry out these experiments at four different mixing times (1 ms, 10 ms, 50 ms and 100 ms) since we had no prior idea of the exchange rate. The results of these experiments are shown in Figure 2.3. It is clear that the exchange rate must be slower that 10 ms since we do not see any evidence of an off diagonal intensity (broadened shape) until we reach a 50 ms mixing time. Unfortunately we cannot distinguish a unique cross peak from these spectra on the 400 MHz instrument.

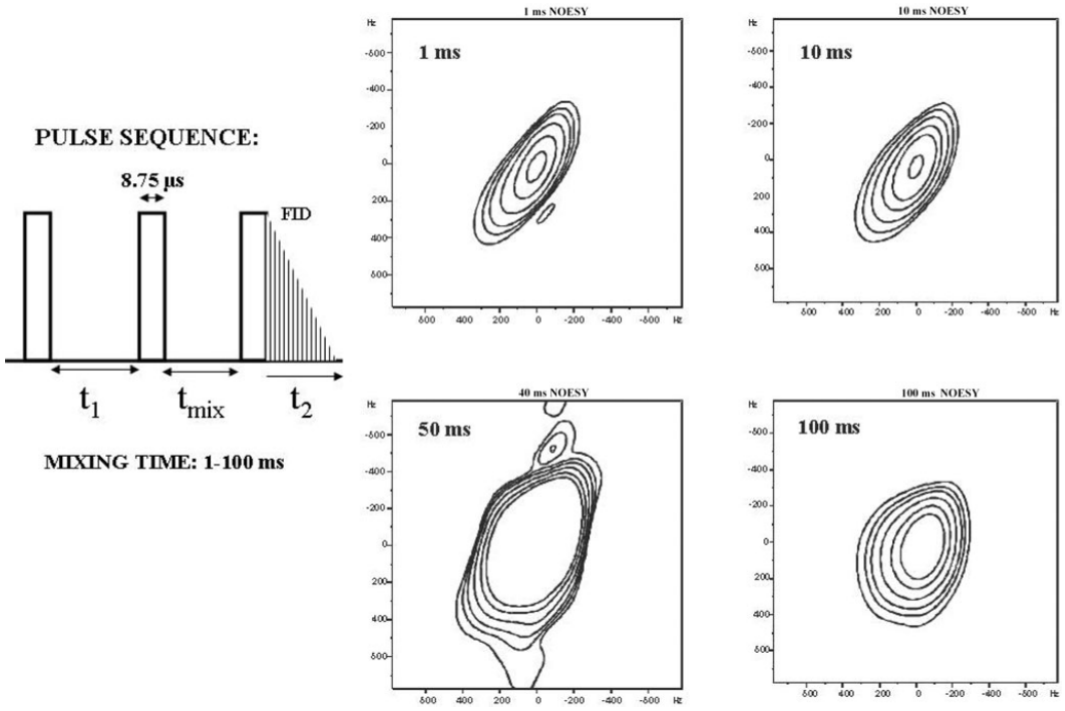


Figure 2.3: 2D exchange NMR spectroscopy of the nitrobenzene/water interface realized in the bead experiment and performed according to the scheme polystyrene/NB/water, shown in Fig. 2.2.

### 2.3.2 Solvatomers of the lithium ion in ‘‘wet’’ nitrobenzene phase

Attempts to realize a high surface area of contact between the water and nitrobenzene phases resulted in broad $^{7}Li$ resonances that, as stated above, led to kinetic exchange data but were not sufficiently resolved to elucidate information on the number of solvatomers involved in the transfer of ions at the liquid-liquid interface. Focus was shifted to study of the “wet nitrobenzene phase”. Wet nitrobenzene is our term for nitrobenzene which has been equilibrated with an aqueous solution of lithium salt. In effect it allows study of the lithium ion after it has transferred form water into the nitrobenzene phase. After equilibrating nitrobenzene with $LiBr_{(aq,saturated)}$ for 3 hours, the experimental clock was set to zero. The $^{7}Li$ NMR spectra were taken at t=0 (see experimental for description of the time scale). The absence of laser light scattering (632.8 nm) indicated that the NB was homogeneous and that there were no microemulsions present, at least on the μm scale. Relatively narrow resonant peaks were obtained for $^{7}Li^{+}$ in pure water ($\Delta Hz_{½} < 1$ Hz) and in dry nitrobenzene ($\Delta Hz_{½} = 10$ Hz) in contrast to the $^{7}Li^{+}$ peak in ‘‘wet’’ nitrobenzene ($\Delta Hz_{½} = 105$ Hz), indicating the presence of multiple solvatomers. (figure 2.1, panel B). It was thought that this broad resonance could become more clearly resolved under the correct experimental conditions to reveal separate solvatomers rather than a single peak. To achieve this, experiments were conducted in a 10mm NMR tube rather than the 5mm tubes which had been used. The increase in volume in the NMR window of observation increases signal to noise but more importantly the increased diameter allowed insertion of a sealed class capilary containing deuterated benzene as an external lock. The solution has no chemical effect on

the system but allows deuterium lock to compensate for magnetic field drifts of the NMR spectrometer.

It has not been recognized in the initial experiments (figure 2.1 B) that the dynamics of this mixed solvation is exceptionally slow, spanning hundreds of hours. It has only been noticed when the NMR spectrum of a one week old sample was compared to the spectrum of the sample taken within 3 h of its preparation. The spectrum taken at t = 3 h shows two well-resolved peaks at ~ 0 ppm and ~ 1.52 ppm (figure 2.4 A.). After 90 h, the peak at 1.52 ppm disappears (figure 2.4 B.). A short, 5 min immersion of the NMR sample in an ultrasonic bath causes the reappearance of a similar peak at 1.14 ppm. (figure 2.4 C). This experiment has been repeated many times, always yielding the reproducible pattern of behavior although the peak separation was slightly different in different sets of experiments. This variability can be attributed to the different amount of sonic energy absorbed by the sample. The observed changes indicate that a reorganization of the solvated lithium ion is taking place on a very slow time scale. We find it quite remarkable that solvent reorganization can be reversed by mechanical disruption. No noticeable changes in the $^{1}$H-NMR spectra taken simultaneously have been observed.

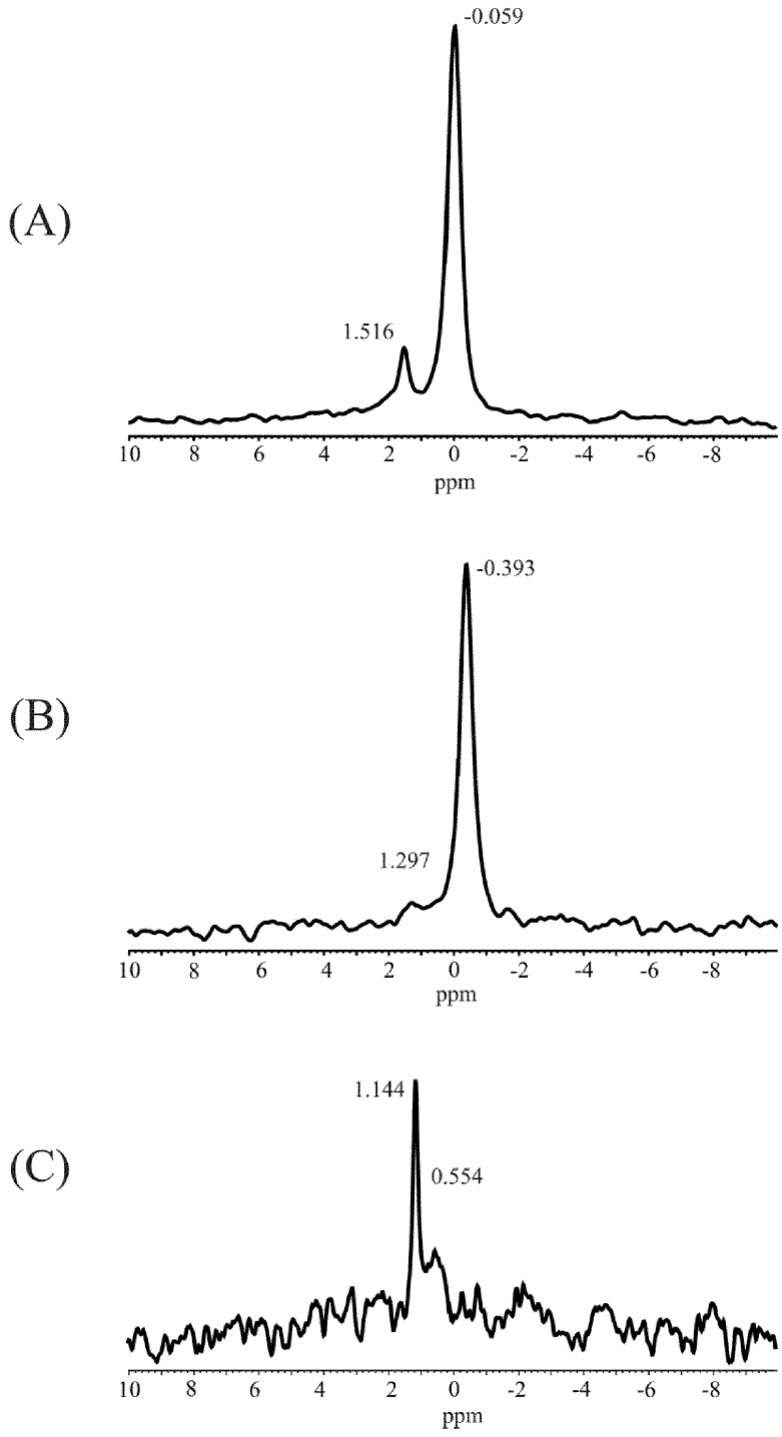


Figure 2.4: Dynamics of the self-organization in $Li^+$/nitrobenzene (water) system. $^7Li$ NMR spectrum in wet nitrobenzene recorded at (A) t = 0 h (20 000 scans), (B) t = 90 h (5500 scans); (C) as in (B), but after sonication for 5 min (12 100 scans).

### 2.3.3 Interaction of lithium ion with glass

Initially, all the experiments were performed in standard 5mm and 10 mm diameter glass NMR tubes. The continuous recording of the spectrum of the $^{7}Li^{+}$ in ‘‘wet’’ NB revealed an interesting experimental artifact. After four weeks of storage in the glass NMR tube, the $^{7}Li^{+}$ peak broadened and could no longer be restored into the original two peak pattern by sonication or by reflux. The $Li^{+}$ assumed some ‘‘immobile’’ form and virtually disappeared from the solution. Moreover, the concentration of $Li^{+}$ in that NB solution dropped below the detection limit (i.e. $< 10^{-6}$ M) of the atomic absorption spectroscopy analysis. The cumulative spectra acquired over 20 000 scans of the empty glass NMR tube, or of the probe without the NMR tube also produced a broad $^{7}Li$ signal that became indistinguishable from the background (figure 2.5.). The glass NMR tube was then replaced by a quartz NMR tube, and the spectrum of a newly prepared LiBr solution in ‘‘wet’’ NB was acquired. The two peaks of the differently solvated lithium ion were again obtained indicating the presence of $Li^{+}$ in two different solvation environments. The spectra of the solutions stored in Teflon ware have maintained their ‘‘free’’ solution appearance. On the basis of these experiments we conclude that the wall of the glass NMR tube adsorbs the lithium ion. These observations are also corroborated by the fact that the concentration of the lithium ion in solution left in a glass NMR tube dropped below the detection limit of the AAS instrument ($10^{-6}$ M) while the freshly prepared saturated solution of LiBr in ‘‘wet’’ NB could be comfortably determined as $[Li^{+}] = 1.43 \times 10^{-5}$M. Further investigation into lithium incorporation in glass is detailed later in this thesis (chapter 6).

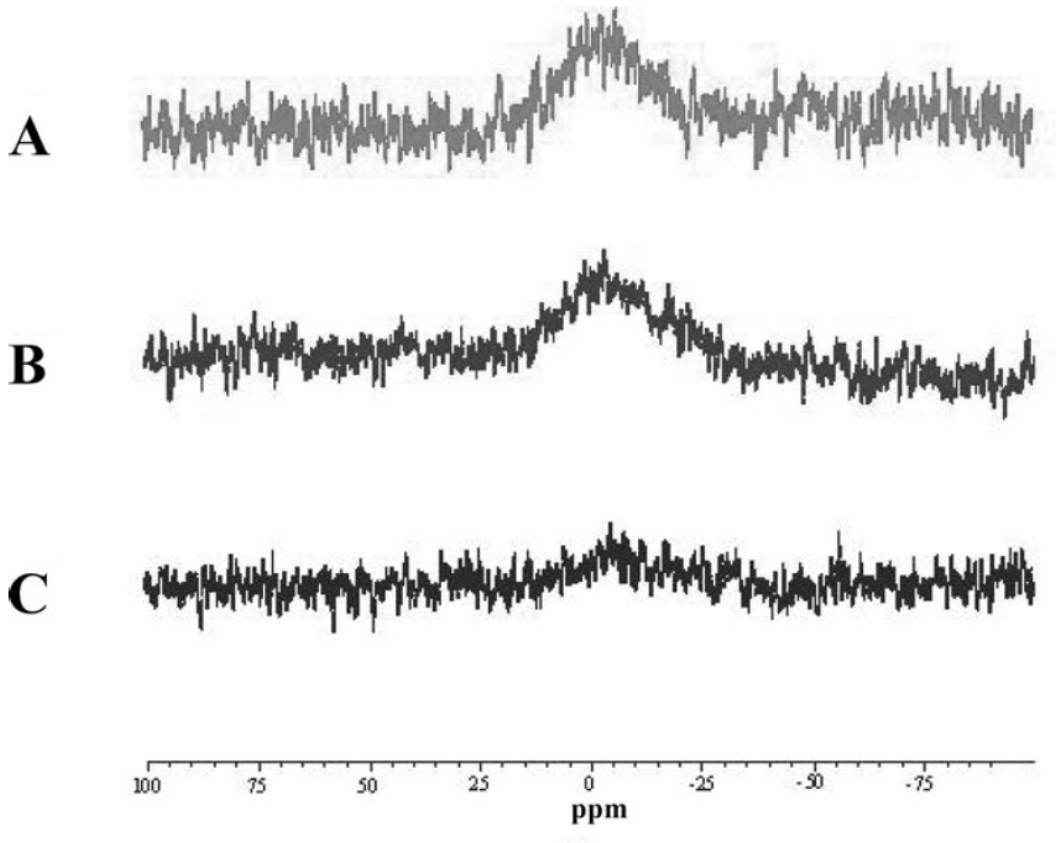


Figure 2.5: NMR spectrum of the $Li^+$ present in the walls of the NMR tube and in the glass enclosure of the NMR probe. 20 000 scans have been acquired. (A) $^7$Li-NMR spectrum of glass NMR tube filled with pure nitrobenzene; (B) $^7$Li NMR spectrum of the ‘‘empty’’ 10 mm glass NMR tube; (C) $^7$Li-NMR spectrum of the ‘‘empty’’ NMR probe. The weak $^7$Li signal is coming from the glass of the probe. Each spectrum represents 10 000 scans.

### 2.3.4 $^{7}LiClO_4$ resonances in water, nitrobenzene and wet nitrobenzene

Numerous studies have proposed that ions must be considered as a hydrated species on transferring across the water/nitrobenzene interface.[41-44] As such, it is likely that the anion identity influences the water environment in the organic phase. The average hydration numbers of $Li^+$, $Br^-$ and $ClO_4^-$ in nitrobenzene have been determined experimentally as 6.0, 2.1, and 0.2 respectively.[20] As such, the slow (up to 1 week) ordering of water in nitrobenzene by lithium, as reported in section 2.3.2 may be reliant on prescence of a hydrophilic anion such as $Br^-$. To study this idea, analogous experiments to those detailed above were conducted with $LiClO_4$ in place of LiBr. The first point of interest is that concentration of lithium species, as determined by atomic absorption, is $9.52 \times 10^{-4}$ M for lithium perchlorate and $1.43 \times 10^{-5}$ for Lithium Bromide. This makes appreciable signal to noise easier to obtain in the $^{7}Li$ NMR spectra. Indeed, whereas in the case of LiBr, it was necessary to co-add several thousand scans, with $LiClO_4$, $^{7}Li$ resonances were clearly observable with as few as 64 scans. This gave the possibility of obtaining kinetic information on solvation rearrangement, since less time is needed for acquisition of each spectrum.

NMR spectra of $^{7}LiClO_4$ in (1) dry NB (1.271 ppm), (2) wet NB (1.025 ppm), (3) 20mM aqueous salt solution (0.375 ppm) and (4) saturated $LiClO_{4(aq)}$ (0.000 ppm) are shown in figure 2.6. The shift in chemical resonance between 1 and 2 is small and suggests that lithium in wet nitrobenzene is solvated mostly by nitrobenzene. As predicted, addition of $LiClO_4$ to the wet nitrobenzene system does not lead to spontaneous formation of multiple solvation states as addition of LiBr had. This

corroborates the hypothesis that a hydrophilic anion such as $Br^-$ contributes to ordering of water in nitrobenzene where more hydrophobic ions such as $ClO_4^-$ are less successful. The difference in resonance between spectra 3 and 4 is attributed to the strong dependence of chemical shift on activity coeffient of the NMR active nuclei. It should be noted that resonance 2, wet nitrobenzene, at 1.025 ppm is broader than the other resonances, suggesting a range of solvatomers of type $Li(H_2O)_x(NB)_y$. Since NMR spectra of $^7Li$ in dry NB and in purely aqueous solution are not discussed various species are denoted by the subscripts as follows: $Li_{(NB)}$ means lithium ion in "wet" nitrobenzene but solvated by a majority of nitrobenzene. $Li_{(NB/W)}$ means mixed solvatomer of lithium ion solvated by both nitrobenzene and water and $Li_{(W)}$ means lithium ion still in wet nitrobenzene phase but solvated in majority by water.

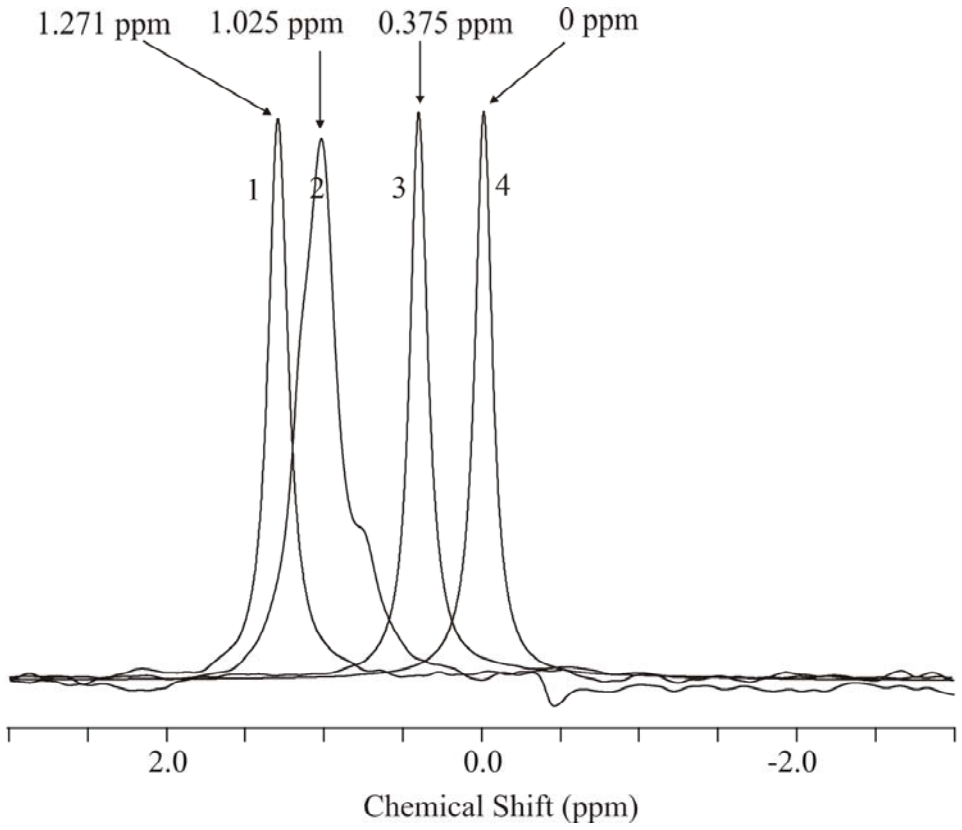


Figure 2.6: $^{7}Li$ NMR spectra of $^{7}LiClO_4$ in (1). Dry nitrobenzene. (2) Wet nitrobenzene. (3) Water (20mM salt concentration). (4) saturated $LiClO_{4(aq)}$ .

### 2.3.5 Inducing multiple $Li^+$ solvation states

Since addition of $LiClO_4$ to wet nitrobenzene did not result in appearance of multiple $^7Li$ resonances, it was an ideal opportunity to assess whether or not these ordered water species as observed with LiBr could be induced by alternative methods. We found two ways to produce metastable lithium solvatomers in wet NB solution: by rapid cooling and by addition of a small amount of the aqueous phase. In the latter, 3 ml of solution of $LiClO_4$ in wet NB (initial solution) was shaken with a small amount (5μl) of water. The $^7Li^+$ spectrum was recorded within 5 minutes of preparation and a second resonance appeared at 0.818 ppm (figure 2.7 A), which is reminiscent of the $Li_{NB/W}$ water solvatomer from the studies of LiBr. When 5 μL of $LiClO_4$ (aq, 1 mM) was added to the initial sample a third solvatomer of lithium appeared at 0.460 ppm (figure 2.7 B), which can be viewed as lithium ion solvated mostly by water, $Li_W$. Figure 2.7 C. shows the effect when the sample initially equilibrated at 298K was cooled to 290K in the NMR probe. In this case the most downfield (1.163 ppm) and intermediate (0.776 ppm) peaks are present. No samples scattered laser light (632.8 nm) after addition of aqueous phase or after cooling, indicating that solutions were homogeneous on the μm scale.

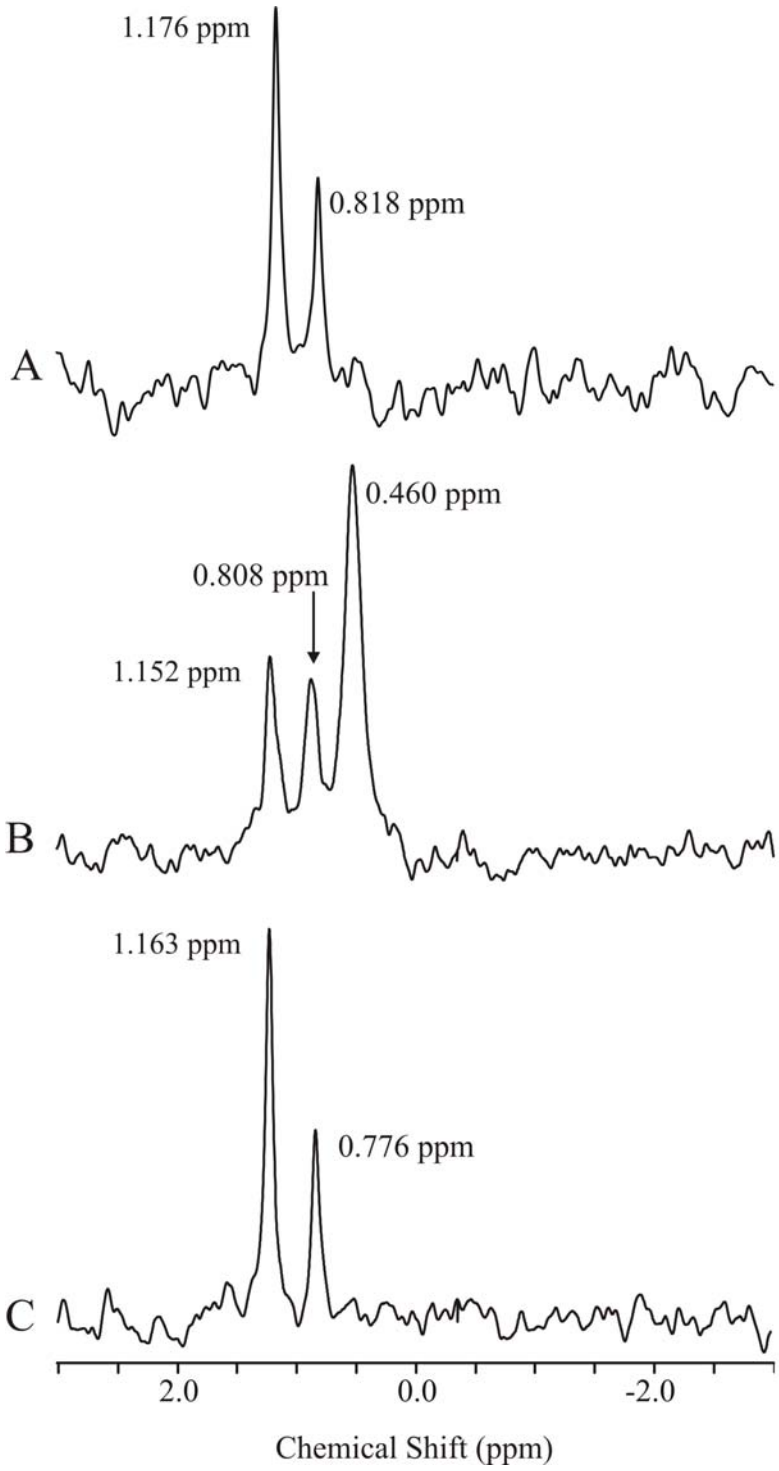


Figure 2.7: $^{7}Li^{+}$ spectra of (A) $LiClO_4$ (wet NB) with 5µl D.I water added. (B) 5µl of $LiClO_{4(aq,\ 1mM)}$ added. (C) cooled to 290K.

### 2.3.6. Kinetic study of $LiClO_4$ (wet NB) cooled to 290K

In order to follow the kinetics of solvatomer transformations, $^7$Li peaks were observed over a period of 15 hrs after $LiClO_4$ in wet NB was cooled from 298K to 290K. Successive NMR spectra were recorded as described above. It is clear from Figure 2.8 spectrum A that three primary solvatomers exist. The downfield peak at 1.165 ppm is near identical in chemical shift to that of $LiClO_4$ dissolved in dried nitrobenzene. Therefore, this solvatomer must consist of lithium solvated mostly by nitrobenzene, $Li_{NB}$. The small peak at 0.379 ppm has a similar chemical shift to that of 20mM $LiClO_4$ in $H_2O$. This solvatomer therefore likely represents lithium solvated in majority by water, $Li_W$. The peak at 0.776 ppm is a solvatomer comprising of lithium solvated by some ratio of both nitrobenzene and water. This solvatomer will be referred to as $Li_{(NB/W)}$. The change in relative intensities of the intermediate and upfield peaks suggest that lithium in the mixed solvation state seems to exchange its mixed solvation sphere for one dominated by water.

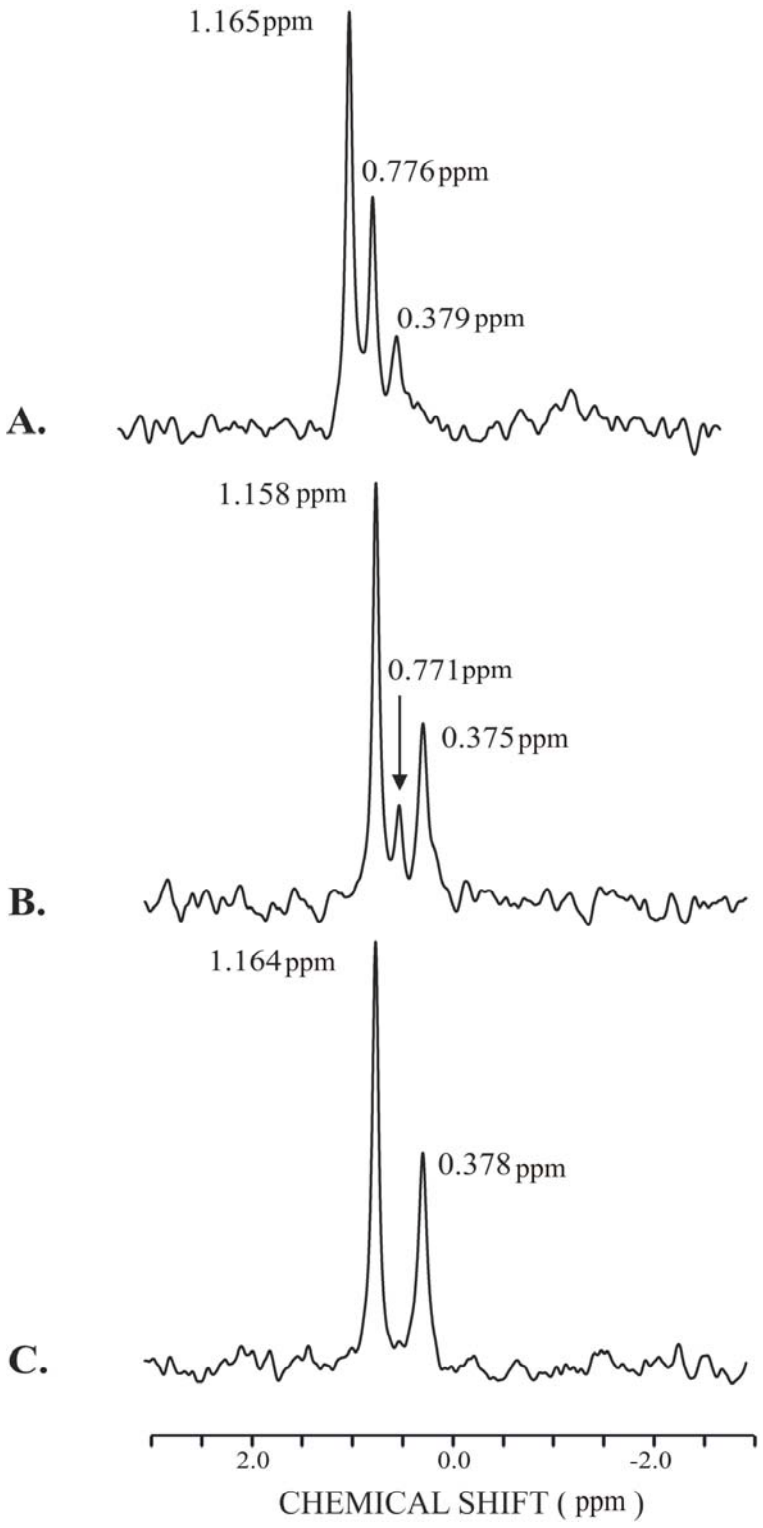


Figure 2.8: $^{7}Li$ NMR spectra of $LiClO_4$ (wet NB) cooled in the NMR probe to 290K. (A) T = 0. (B) 310 min. (C) 806 min.

The results of the 15 hr kinetic experiment are summarized in Figure 2.9. Plot A is the plot of the sum of all three peak areas seen in Fig. 2.8. The sum is constant indicating that the total lithium species in the NMR active region of the sample tube does not decrease over the 15 hr period. This is not a trivial statement in view of the incorporation of $Li^+$ into glass (documented in more detail in chapter VI). The increase in the area of the most downfield peak (1.165 ppm, Fig. 2.8) corresponding to the solvatomer $Li_{(NB)}$ is shown in plot B. ln (peak area) vs. time is linear for plot B, therefore the increase in concentration of Li $_{(NB)}$ solvatomer obeys first order kinetics with rate constant, $k = 3 \times 10^{-6}$ $sec^{-1}$. The increase in the area of the most upfield peak (0.379 ppm, figure 2.8) corresponding to $Li_{(W)}$ is shown in plot C. The decrease in the area of the intermediate peak (0.776 ppm, figure 2.8) corresponding to $Li_{(NB/W)}$ is shown in plot D. Since ln (peak area) vs. time is linear for plot D, the decrease in concentration of Li $_{(NB/W)}$ solvatomer obeys first order kinetics with rate constant, $k = 7 \times 10^{-5}$ $sec^{-1}$. Taking an endpoint of the kinetic experiment as 651 min., the peak areas corresponding to $Li_{(NB)}$, $Li_{(NB/W)}$ and $Li_{(W)}$ solvatomers were calculated as a percentage of total peak areas. At the end of the 15 hr period, the lithium species exist as 57.6 % $Li_{(NB)}$, 2.3 % $Li_{(NB/W)}$ and 40.2 % $Li_{(W)}$.

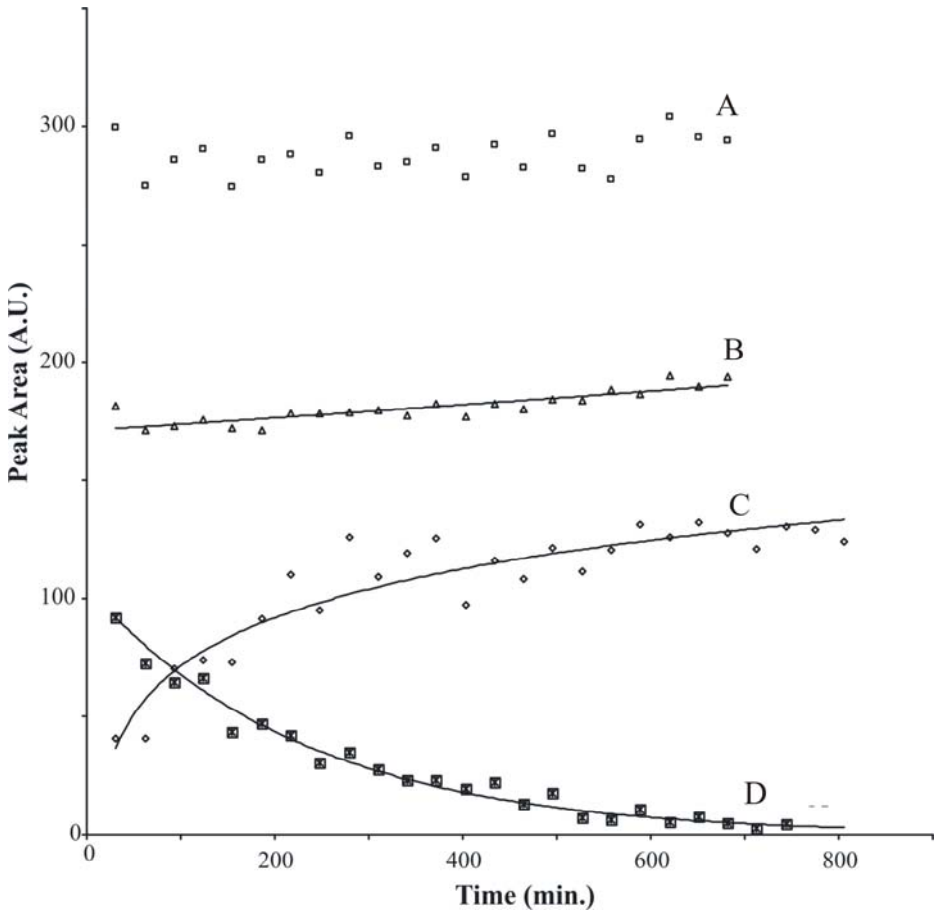


Figure 2.9: Plot of peak area vs. time for the solvatomers produced when $LiClO_4$/wet NB system is cooled to 290K and followed by $^7Li$ NMR over 15 hours. (A) Sum of peak areas of $Li_{(NB)}$, $Li_{(NB/W)}$ and $Li_{(W)}$ solvatomers. (B) Growth in concentration of the $Li_{(NB)}$ solvatomer. (C) Increase in concentration of the $Li_{(W)}$ solvatomer. (D) Decrease in concentration of the $Li_{(NB/H2O)}$ solvatomer.

### 2.3.7 Effect of vessel wall on kinetics

All experiments decribed thus far were performed in 5 mm and 10mm diameter glass NMR tubes. It was therefore deemed important to investigate whether the direct contact between the solutions and glass wall had an effect on $^{7}Li$ resonances observed. $LiClO_4$ in wet nitrobenzene was cooled to 285K in the NMR spectromer. For this experiment, the solution was contained within a Teflon tube liner inserted in the 5mm sample tube. Fig. 2.10 A and B show the spectra at t = 0 and t = 12hrs. It is clear that without access to glass wall, the solvatomer $Li_W$ previously observed at ~ 0.4 ppm does not exist. Over the 15 hr period, the relative intensities of the peaks at 1.181 and 0.796 ppm reverse. The intermediate solvatomer $Li_{(NB,W)}$ is metastable. In the absence of the vessel wall, this metastable intermediate solvatomer relaxes back to a lower energy $Li_{(NB)}$ solvatomer. Taking an endpoint of the kinetic experiment as 620 min., the peak areas corresponding to $Li_{(NB)}$, $Li_{(NB/W)}$ and $Li_{(W)}$ solvatomers were calculated as a percentage of total peak areas. At this point, the lithium species exist as 54.6 % $Li_{(NB)}$, 45.4 % $Li_{(NB/W)}$ and 0 % $Li_{(W)}$. Comparison of cooling experiments with and without Teflon tube liner suggests that the glass wall of the NMR tube appears to assist the condensation of the $Li_{(W)}$ solvatomer.

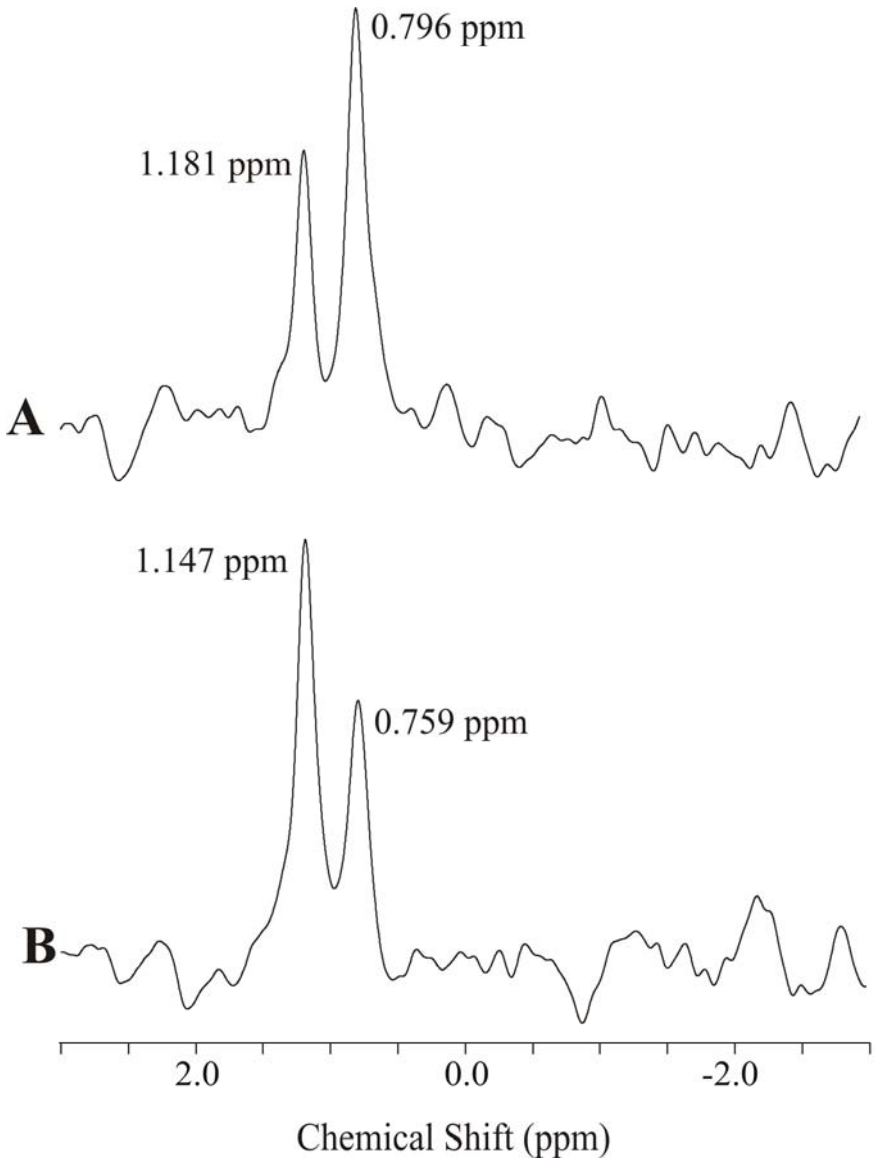


Figure 2.10: $^{7}Li$ NMR spectra of $LiClO_4$/ wet NB cooled in the NMR probe to 285K in 5mm NMR tube with Teflon tube liner. (A) T = 0. (B) T = 930 min.

# CHAPTER III

# $^2$D NMR STUDY OF LITHIUM SALTS IN $D_2O$-SATURATED NITROBENZENE

## 3.1 Introduction

The experiments described in chapter two were conducted with $^7$Li as the NMR active nucleus. As such, solvatomers of $Li^+$ were observed as separate resonances in the $^7$Li spectrum, depending on the relative contributions of water and nitrobenzene to the lithium solvation shell. It was determined that three distinct solvation environments are observable through $^7$Li NMR. These are lithium solvated in majority by nitrobenzene, $Li_{NB}$, lithium solvated by a mixture of nitrobenzene and water $Li_{NB/W}$ and lithium with majority water in its solvation shell $Li_W$. The limitation of this approach is that since lithium *is* the NMR nucleus, it is impossible to determine the effect lithium has on water environment since we cannot conduct a $^7$Li NMR experiment without the lithium present. An alternative approach is to conduct NMR on the water itself using deuterium as the NMR-active nucleus, allowing comparison of the water environment in nitrobenzene with and without the addition of lithium species.

The hydrodynamic radii of various ions has been estimated from consideration of crystallographic radii and hydration numbers derived from Karl Fischer titration.[20] Described in this chapter is the use of $^2$H NMR to gain further insight into the dynamics of the solvation environment of $Li^+$ in the mixed $Li^+$/nitrobenzene/water system. The use

of deuterium as a reporter instead of lithium means that a comparison can be made between NB/W solutions with and without lithium species. Diffusion ordered spectroscopy (DOSY) was used to determinate the hydrodynamic radii of the lithium ion in the $Li^+$/nitrobenzene/water system. This technique has not been possible with $^7Li$ NMR since the concentration of LiBr in the water-saturated nitrobenzene is 1 x $10^{-5}$ M, which is too low to obtain DOSY spectra.

## 3.2 Experimental

### 3.2.1. Materials

Lithium perchlorate (≥99%, Aldrich) and Lithium bromide (≥99%, Aldrich) were used as received. Nitrobenzene (99%, ACROS Organics) was redistilled under vacuum and dried before use by molecular sieves (4A, Sigma–Aldrich). Glass 5mm and 10mm NMR sample tubes were obtained from Wilmad-Lab glass. All water used was de-ionized to 18 MΩ using a US-Filter Modulab water system (US Filter, Warrendale, PA). Deuterium oxide (Cambridge Isotope Laboratories, 99.9% D) was used as received.

### 3.2.2 Procedures

Saturated aqueous solutions of $LiClO_4$ and LiBr were prepared by adding $LiClO_4$ to $D_2O$ until solid salt remained. For preparation of ‘‘wet’’ NB solution of $LiClO_4$ and LiBr, lithium salt was added to $D_2O$ until saturated. This saturated aqueous solution was

then stirred with vacuum distilled nitrobenzene for three hours and then allowed to separate for one hour. When the clear NB phase was pipetted from the equilibrating mixture, the experimental clock was set to t =0. The lithium content of the "wet" NB solution has been determined by atomic absorption spectroscopy to be 9.52 x $10^{-4}$ M for Lithium Perchlorate and 1.43 x $10^{-5}$ for Lithium Bromide. The published concentration of water in water-saturated ‘‘wet’’ NB is between 170 and 190mM.

### 3.2.3. NMR experiments

The 1D NMR spectra were recorded using a Bruker AMX-400 spectrometer (Bruker BioSpin, Rheinstetten, Germany) with a 10 mm broadband probe. $^{2}$H-NMR spectrum of saturated (6M) $LiClO_4$ in $D_2O$ was recorded before each experiment and the corresponding signal calibrated to 0 ppm. For the kinetic data, peak areas were calculated by a line fitting function of the Mestre-C NMR software **(**Mestrelab Research SL, Santiago de Compostela University, Santiago, Spain**).** The line fit function uses the Levenberg-Marquardt non–linear least squares and Downhill Simplex (Nelder and Mead) algorithms for estimating peak parameters (position, intensity, line width and line shape function). Temperature of the NMR probe was controlled to an accuracy of ±1 K using the spectrometers VT accessories. No field frequency lock was used during the data acquisition. $^{2}$D-DOSY experiments were recorded using a Bruker DRX-500 spectrometer (Bruker BioSpin, Rheinstetten, Germany) with a 5 mm broadband probe with z gradients.

## 3.3. Results

### 3.3.1 Effect of lithium perchlorate on $^2$H chemical shift

The effect of $LiClO_4$ on the ordering of water in nitrobenzene was studied by a simple 1D $^2$H NMR experiment (figure 3.1). Pure $D_2O$ was calibrated to 0 ppm then two spectra were recorded in succession: spectrum 1 (solid black line) is the $^2$H NMR spectrum for nitrobenzene saturated with $D_2O$. Spectrum 2 (dashed line) is the $^2$H NMR sprectrum for nitrobenzene equilibrated with 6M $LiClO_4$ in $D_2O$. Both experiments were repeated 5 times with observed chemical shift differences of less than 0.005 ppm. This confirms that the downfield shift after addition of $LiClO_4$ is a real result rather than a drift in the magnetic field of the instrument. This shift of the $^2$H resonance towards 0 ppm suggests an increase in water ordering leading to a $^2$H resonance that resembles that of bulk $D_2O$.

### 3.3.2 Effect of cooling on $^2$H spectrum

At room temperature, a solution of $LiClO_4$ in water-saturated nitrobenzene gives a single, clearly resolved resonance in a 1D $^7$Li spectrum. This species is hypothesized to be lithium ion with a solvation sphere dominated with nitrobenzene. Upon cooling from 298K to 290K, a second resonance appears in the $^7$Li spectrum that has been attributed to a higher energy metastable water aggregate, with a mixed solvation shell of water and nitrobenzene $Li_{W/NB}$. This solvatomer is metastable and slowly decays over period of tens

of minutes. In the presence of glass it forms a stable species $Li_W$, which contains mostly water and which is nucleated by the hydrophilic glass surface. In the absence of glass surface (i.e. in a Teflon lined NMR tube) it converts to the nitrobenzene solvated species, $Li_{NB}$ . Figure 3.2 shows the effect of this cooling process on $^2H$ chemical shift for nitrobenzene stirred with a saturated solution of $LiClO_4$ in $D_2O$. Spectra A and B are $D_2O$ in nitrobenzene (termed wet nitrobenzene) at 289K and 290K, respectively. Spectra C and D are $LiClO_4$ in wet nitrobenzene at 298K and 290K respectively. The cooling of both solutions results in the subtle shift (0.03 ppm) of the $^2H$ chemical shift downfield, towards 0 ppm (chemical shift of pure $D_2O$ calibrant), indicating that the water species take on increasing bulk water character. This suggests that in both solutions there is an aggregation of water upon cooling. It is interesting to note that the chemical shift difference upon addition of lithium ion (0.95 ppm, figure 3.1) is large in comparison to that caused by cooling. This is in direct support of FTIR data (chapter IV) which suggests the ordering of water promoted by $Li^+$ is large in comparison to that caused by cooling.

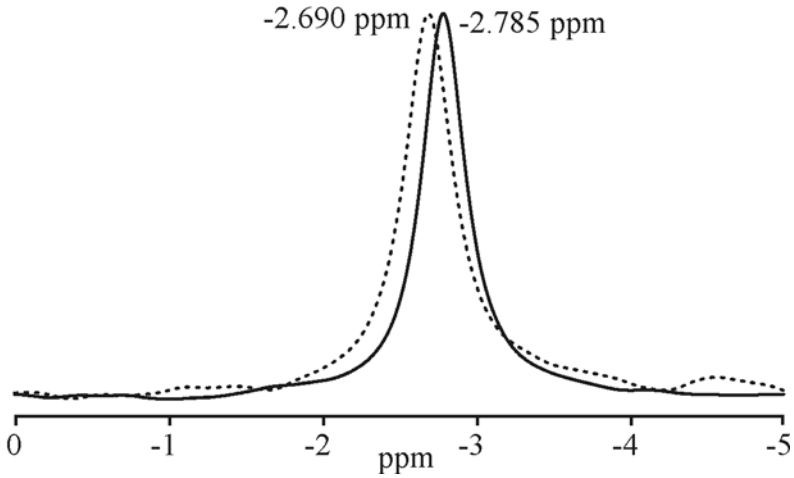


Figure 3.1: $^{2}H$ NMR spectrum of nitrobenzene saturated with $D_2O$ (black line) and nitrobenzene saturated with $LiClO_4$ in $D_2O$ (6M) (dashed line)

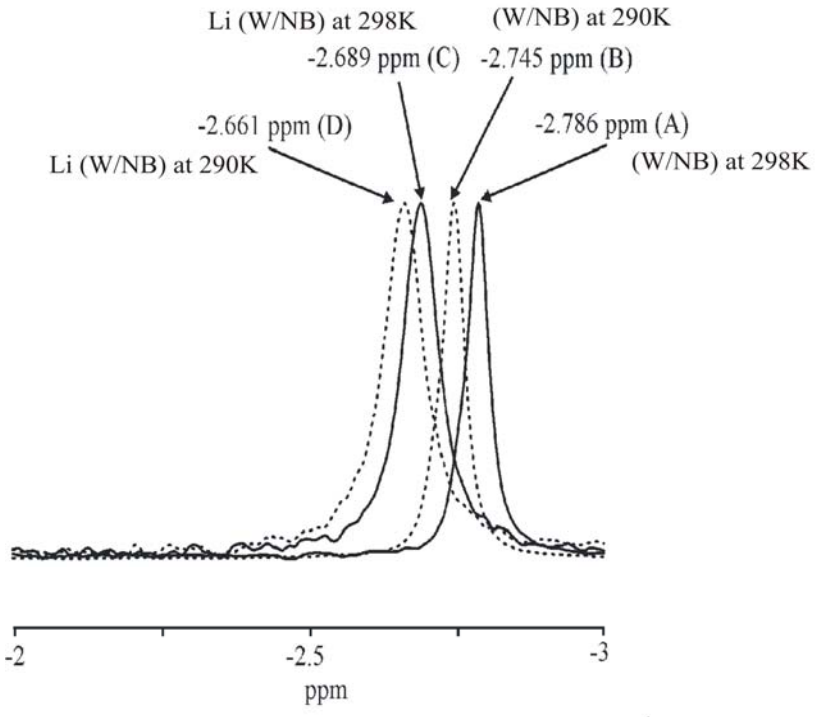


Figure 3.2: (A) $^{2}H$ NMR spectrum of (A) nitrobenzene saturated with $D_2O$ (black line) and (B) 290K (dashed line), (C) nitrobenzene saturated with $LiClO_4$ ($D_2O$) at 298K (D) 290K.

However, cooling does not result in the occurrence of multiple resonances as seen in the $^{7}$Li NMR spectrum (figure 3.3). It is important to remember that this is the same experiment only using a different 'reporter species'. The apparent discrepancy in this result can be explained by considering the abundance of these reporter species .When the cooling experiment is performed and followed by $^{7}$Li NMR (figure 3.3), the solution evidently becomes supersaturated with water, and becomes microheterogeneous, i.e the decrease in temperature causes droplets of water to form. These results indicate that lithium partitions into this phase resulting in two 'solvatomers', the solvatomer consisting of lithium solvated in majority by nitrobenzene (1.163 ppm), and the solvatomer which results from cooling and resembles lithium solvated by a mixed solvation shell, $Li_{NB/W}$ (0.776 ppm). The water droplets that form after a modest temperature drop of 8 K are a small fraction of the overall water content of nitrobenzene. It is for this reason that in the case of $^{2}$H spectrum (figure 3.2B) the second solvatomer is unobservable. Conversely with $^{7}$Li, the lithium species preferentially solvate with the newly formed species, thus 'illuminating' this second, metastable, water-rich solvatomer $Li_{W/NB}$.

### 3.3.3 Addition of bulk water to system

In previous $^{7}$Li NMR experiments, it was found that cooling of the $LiClO_4$/nitrobenzene/water system resulted in formation of multiple solvatomers (Figure 3.3). In this case, the water content of the wet nitrobenzene is ~200 mM, compared to a

$LiClO_4$ concentration of 9 x $10^{-4}$ M. It is therefore clear that water dissolved in nitrobenzene is in great excess of lithium species.

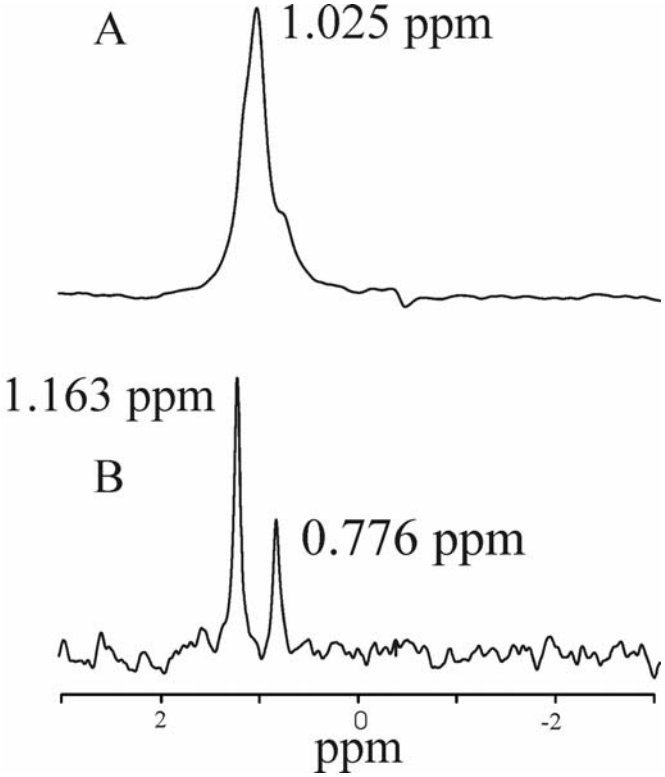


Figure 3.3: $^{7}Li$ NMR spectra of nitrobenzene saturated with $LiClO_4$ in $D_2O$ at (A) 298K and (B) 290K

In the recent $^{2}H$ NMR studies, the formation of these multiple solvatomers is undetectable due to the strong resonance of the dissolved deuterium. Previous studies also determined that the same effect as cooling could be observed by addition of a small amount of water to the solution on the surface of a wet glass capilary. It was proposed that the concentration of the ordered water species could be enhanced to the point of detection by such methods. To the initial $LiClO_4$/wet nitrobenzene system an additional 5 μL of $D_2O$ was added on the surface of a glass capilary. Figure 3.4 A,B,C below shows the kinetics of solvatomer transformation at t = 0 (insertion of wet glass capilary), t = 90 minutes and t = 180 minutes, respectively. It is clear from Figure 3.4 spectrum C that three primary solvatomers exist. Pure $D_2O$ is assigned to 0 ppm. Nitrobenzene containing $LiClO_4$/$D_2O$ gives a single resonance at ~-2.7 ppm. It is therefore clear that the downfield peak at -0.316 ppm is a mixed solvation shell with nitrobenzene and water. Conversely the peak at -2.710 ppm represents a species almost entirely solvated by nitrobenzene. The shoulder which grows at 0.040 ppm is consistent with $^{7}Li$ NMR results and represents a large water aggregate nucleated at the glass capilary surface. The change in relative intensities of the three peaks suggest that the solvatomer formed immediately on addition of 5 μL $D_2O$ is metastable and appears to exchange its mixed solvation sphere for one dominated by water (0.040 ppm) and one dominated by nitrobenzene (-2.704 ppm). This is in direct agreement with the analogous $^{7}Li$ experiments as reported in chapter 2.

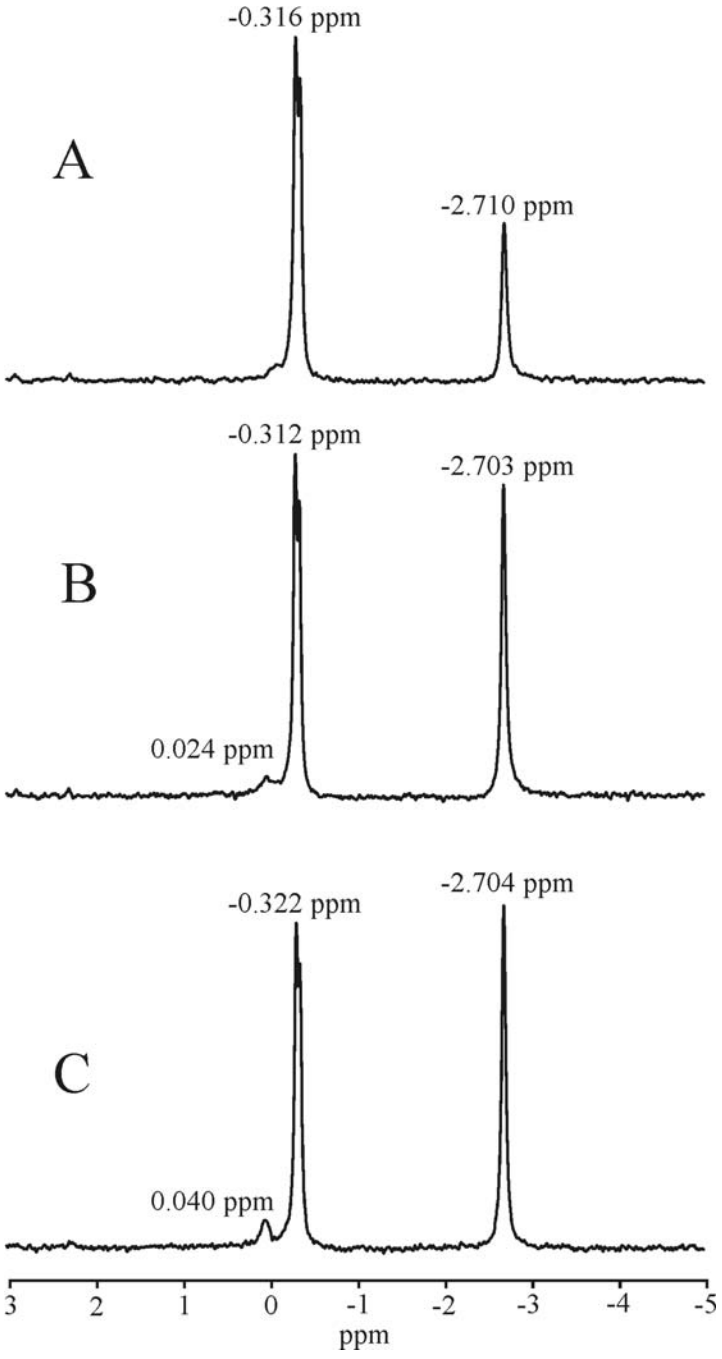


Figure 3.4: $^{2}H$ NMR spectra of $LiClO_4$ (wet NB) with 5μL of $D_2O$ added and shaken. (A) T = 0. (B) 90 min. (C) 180 min.

The results of these experiments are summarized in Fig. 3.5. A is the plot of the decrease in the area of the peak at ~ -0.3 ppm (Figure 3.4) corresponding to $Li_{(NB/W)}$. For this species, the logarithm (peak area) vs. time is linear, therefore the decrease in concentration of $Li_{(NB/W)}$ solvatomer obeys first order kinetics with rate constant, $k = 4 \times 10^{-5}$ $sec^{-1}$. The increase in the area of the most upfield peak (~-2.7 ppm, Figure 3.4) corresponding to $Li_{(NB)}$ is shown in plot B. The increase in the area of the most downfield peak (0.040 ppm, Figure 3.4) corresponding to $Li_{(W)}$ is shown in plot C. The increase in peak areas shown in plots B and C do not follow first order kinetics. On decay of the metastable $Li_{(NB/W)}$ species, there is clearly a subsequent transport of water followed by incorporation of this water into the $Li_{(W)}$ and $Li_{(NB)}$ species. The two superimposed processes make kinetics difficult to interpret.

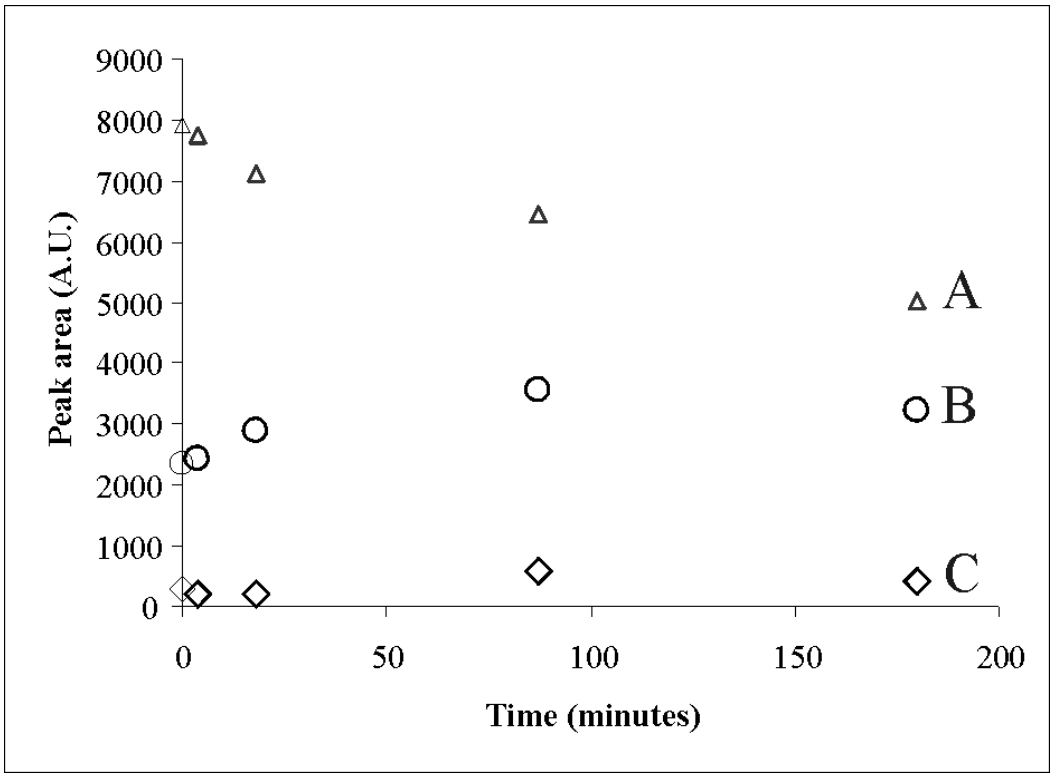


Figure 3.5: Plot of peak area vs. time for the solvatomers produced when 5 μL of $D_2O$ is added to $LiClO_4$/wet NB system, followed by $^2H$ NMR over 180 minutes. (A) Decrease in concentration of the $Li_{(NB/W)}$ solvatomer. (B) Increase in concentration of the $Li_{(NB)}$ solvatomer. (C) Increase in concentration of the $Li_{(W)}$ solvatomer.

### 3.3.4 DOSY Studies

Table 3.1 shows the effect of lithium species on the diffusion coefficient of $D_2O$ in nitrobenzene. Diffusion coefficients were obtained from pulse field gradient, diffusion ordered spectroscopy (DOSY) experiment. The diffusion coefficients were measured for the $^2H$ resonance at ~-2.7 ppm, corresponding to the $Li_{(NB)}$ solvatomer and at ~ - 0.3 ppm, corresponding to the $Li_{(W/NB)}$ solvatomer. The resulting hydrodynamic radii, $r_h$, were calculated from the Stokes-Einstein equation.[45]

$$D = KT / 6\pi\eta r_h$$

Where D is the diffusion coefficient for the species, ($m^2\ s^{-1}$) K is the Boltzmann constant ($1.3807 \times 10^{-23}\ m^2\ kg\ s^{-2}\ K^{-1}$), $\eta$ is the viscosity of the medium ($8.94 \times 10^{-4} kg\ m^{-1}\ s^{-1}$ for nitrobenzene) and $r_h$ the hydrodynamic radius of the species (m). Somewhat surprising is the finding that the ordering effect of lithium on water in nitrobenzene, does not result in a significant increase of the hydrodynamic radii for the solvatomer $Li_{NB}$ at ~-2.7 ppm. The diameters of the hydrated species in nitrobenzene are all smaller than that found for bulk water, which has a self-diffusion coefficient of $2.13 \times 10^{-9}\ m^2 s^{-1}$ and $R_h$ of 1.5 Å. This is intuitive since the decreased hydrogen bonding between water molecules in a hydrophobic medium reduces the hydrodynamic radius versus that of bulk water. However, the fact that lithium does not increase the hydrodynamic radius significantly is surprising.

Addition of lithium to the wet nitrobenzene (observed in the $^{2}H$ experiments at ~ -2.7 ppm, figure 3.4) may result in an increase in hydrogen-bonding of the water dissolved in nitrobenzene. $^{7}Li$ NMR results of LiBr in wet nitrobenzene (chapter II) suggest that lithium can order water to the point that a second clear solvatomer is observed, $Li_{NB/W}$, which is proposed to be an aggregate of water molecules within the nitrobenzene. However, this does not mean that the solvatomer $Li_{NB}$ ($^{2}H$, -2.7 ppm, figure 3.4) should experience an increase in size, observed as a decrease in mobility observed by diffusion spectroscopy (DOSY). As such, the failure of lithium to increase the hydrodynamic radii of the solvatomer at ~-2.7 ppm in the $^{2}H$ spectra, does not contradict the earlier $^{7}Li$ experiments. It is possible that in the case of the $Li_{NB}$ solvatomer, addition of lithium does not lead to 'pockets' of isolated hydrated species in the organic phase, but moreover a network of H-bonded water homogenously dispersed throughout the nitrobenzene. We propose here that addition of lithium species to wet nitrobenzene increases hydrogen bonding but not, as first thought, resulting in aggregates of hydrated lithium but in a hydrogen bonded network of water molecules. This hypothesis explains the fact that hydrodynamic radii elucidated from DOSY are small, on the order of single water molecules. A simple calculation of the Loschmidt's number for lithium (ions per $cm^{3}$) reveals an inter-atomic separation of ~ 100 Å for the lithium cations, making it feasible that $Li^{+}$ orders water through hydrogen bonding of its multiple solvation shells. Further evidence that $Li^{+}$ contributes to an increase in water H-bonding was obtained by observing the free -OH stretch of wet nitrobenzene by FTIR (Chapter IV)

DOSY data was also collected for the $^{2}H$ resonance corresponding to the solvatomer $Li_{(NB/W)}$ (-0.316 ppm, figure 3.4), which has a diffusion coefficient of 2.25 x $10^{-9}$ $m^2s^{-1}$ +/- 5 x $10^{-11}$ $m^2s^{-1}$ which is closer to that of bulk water (2.13 x $10^{-9}$ $m^2s^{-1}$). This makes sense, since we know that the peak at -0.316 ppm in the $^{2}H$ spectra results from addition of excess water. We attempted to measure the diffusion coefficient for the "shoulder" peak at 0.040 ppm but the species did not diffuse sufficiently, adding evidence to the hypothesis that this resonance represents hydrated lithium immobilized at the glass capilary.

A second possible explanation for the small change in hydrodynamic radii on addition of $Li^{+}$ could result from a misinterpretation of the DOSY results. When diffusion spectroscopy is used to measure diffusion of water, it is usually not considered that DOSY measures the diffusion of the NMR active nucleus irrespective of whether it truly represents the entire species. In the context of our experiment, it is possible that the diffusion of $^{2}H$ (instead of $D_2O$) is being measured (hence the large value of D) as the deuterium 'hops' from one water molecule to another. This is largely ignored and a good experiment to confirm or deny this would be to compare diffusion studies on both O and H of water. While we have used $^{2}H$ to probe diffusion, $^{17}O$ could also be used to determine if the diffusion coefficients vary for the entire molecule. If the values of D varies, the use of DOSY for study of water diffusion would be hampered by this effect. We do not currently have a sufficiently sensitive instrument for study of $^{17}O$ DOSY, but future studies are desirable.

Table 3.1: Diffusion coefficients and hydrodynamic radii for water species in various nitrobenzene solutions., measured at -2.7 ppm on the $^2H$ NMR spetra.

| **Solution** | **Diffusion coefficient, D ($m^2s^{-1}$)** | **$r_h$, (Å)** |
|---|---|---|
| **Nitrobenzene/$D_2O$** | **$2.3 \times 10^{-9}$ +/- $5 \times 10^{-11}$** | **1.0** |
| **Nitrobenzene/LiBr(D2O)** | **2.5 x 10-$^{9}$ +/- $5 \times 10^{-11}$** | **0.99** |
| **Nitrobenzene/LiClO4(D2O)** | **$2.3 \times 10^{-9}$ +/- $5 \times 10^{-11}$** | **1.0** |

# CHAPTER IV
# FTIR STUDIES OF LITHIUM SALTS IN WATER-SATURATED NITROBENZENE

## 4.1. Introduction

The infrared spectrum of water has been extensively studied both as a pure solvent,[46-51] in solvent mixtures,[52-58] and as a solute in hydrophobic media.[59-62] The water molecule has $C_{2v}$ symmetry and three IR active vibrations.[61] More than three bands are usually present in the IR spectrum of water due to the occurrence of combination, librational and overtone bands. The IR band which represents the bending mode (n2) of water usually appears in the region 1595-1650 $cm^{-1}$. This band is not sufficient to elucidate the molecular state of water without considering the remaining modes of water.[61] Conversely, the stretching vibrational modes of water have been used to study the molecular state of water where water is the solute in a hydrophobic solvent,[61] such as the water/nitrobenzene system in this work. The IR bands corresponding to the antisymmetric (ν3) and symmetric (ν1) stretching modes are normally seen at 3000-3800 $cm^{-1}$. The antisymmetric (ν3) and symmetric (ν1) stretching modes have differing positions and intensities depending on the water environment and the association of water molecules through H-bonding.[61] The ν3 and ν1 bands in water vapor absorb at 3756 and 3657 $cm^{-1}$ respectively.[61] The bands absorb at a lower wave number when water interacts with its environment, for example with bulk nitrobenzene in this work. The difference in

the maximum positions of these bands is ca. 100 $cm^{-1}$ for the example of water bound in symmetric complexes, both protons hydrogen bonding. For water dissolved in hydrophobic solvent, especially when the concentration of water is below 1 x $10^{-3}$ M, the ν3 and ν1 bands are clearly two separate absorptions.[61] As the water content increases in less hydrophobic solvents the bands appear to merge and for pure water, a broad band with a maximum at approximately 3300 $cm^{-1}$ is observed.[61] In reality, this broad absorption which is familiar to chemists at the OH peak is comprised of the ν3 and ν1 bands that broaden considerably due to the hydrogen bonding. It is difficult to elucidate the molecular state of water in nitrobenzene based on the shifts of the stretching bands of water because there is a strong coupling between the ν3 and ν1 bands.[61] However, since $\nu_1$ and $\nu_3$ intensities are intimately related to the extent of hydrogen bonding between water molecules, the effect of lithium salts on aggregation of water through hydrogen bonding can be studied by FTIR.

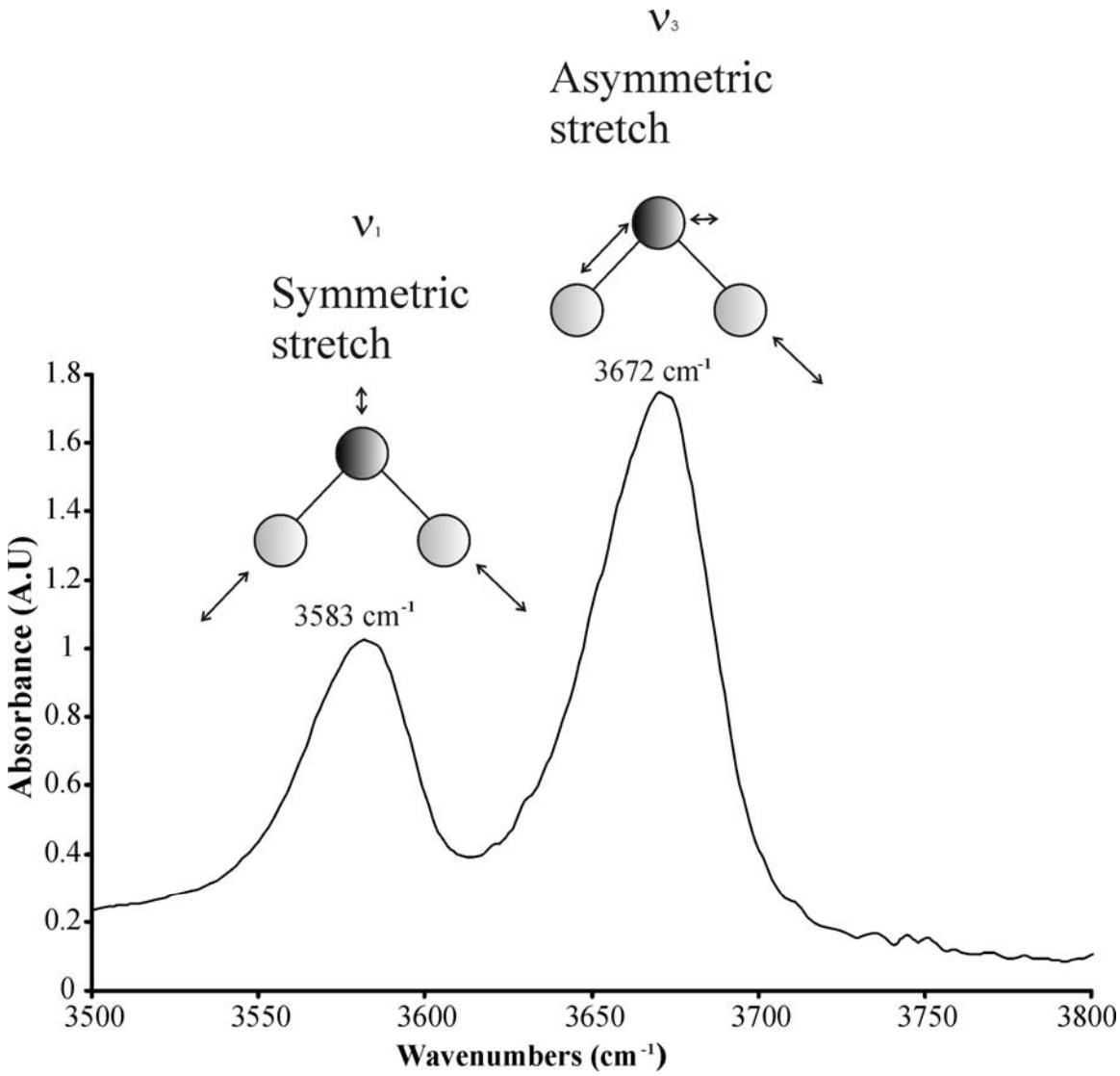


Figure 4.1: Schematic of IR stretches for $H_2O$ molecules and corresponding IR spectrum.

## 4.2 Experimental

### 4.2.1. Materials

Lithium perchlorate and lithium bromide (≥99%, Aldrich) was used as received. Lithium undecamethyl carba-closo-dodecaborate was received from the research group of Professor Josef Michl at the University of Colorado, Denver, Colorado. Nitrobenzene (99%, ACROS Organics) was redistilled under vacuum and dried before use by molecular sieves (4A, Sigma–Aldrich). Glass 5mm NMR sample tubes were obtained from Wilmad-Labglass. All water used was de-ionized to 18 MΩ using a US-Filter Modulab water system (US Filter, Warrendale, PA).

### 4.2.2. Procedures

Saturated solutions of LiBr, $LiClO_4$ and $LiHCB_{11}Me$ in dry nitrobenzene (NB) were prepared by shaking excess of lithium salt with dry NB for 5 minutes and then allowing the mixture to equilibrate for 3 hrs prior to measurement. Saturated solutions of $LiClO_4$ in water were prepared by adding $LiClO_4$ to de-ionized water until solid salt remained. For preparation of ‘‘wet’’ NB solution of LiBr, $LiClO_4$ and $LiHCB_{11}Me$, solid lithium salt was added in excess to NB which had previously been equilibrated with water for 24 hrs. The mixture was shaken for 5 minutes and allowed to equilibrate for 3 hours prior to measurement. When the clear NB phase was pipetted from the equilibrating mixture, the experimental clock was set to t =0.

The lithium content of the "wet" NB solution was determined by atomic absorption spectroscopy to be 9.52 x $10^{-4}$ M. The published concentration of water in water-saturated ‘‘wet’’ NB is between 170 and 190mM.[19]

### 4.2.3. IR Experiments

The FT-IR spectra were recorded using a BioRad FTS 6000 spectrometer (BioRad Laboratories) controlled by WIN-IR pro software (BioRad Laboratories). Samples were injected into a liquid transmission cell (Pike Technologies) with 32 mm x 3 mm circular ZnSe windows (Pike technologies). Pathlength used was 1mm (Teflon spacer, Pike Technologies). Each experiment consisted of 100 added scans, resolution 4 $cm^{-1}$, aperture 2mm. Each experiment was recorded versus a background spectrum of dry NB. For the cooled experiments, the sample cell was placed in the refrigerator for 1 hour until temperature of cell was a stable $10^0$C. The FTIR measurement was conducted with 1 minute of removal from the refrigerator.

## 4.3 Results

The NMR experiments have been complemented by parallel FTIR investigation. Vibration of hydrogen-bonded water (occurring at ~ 3550-3200 $cm^{-1}$, broad[63]) is obscured by strong absorbance by nitrobenzene. The symmetric and asymmetric stretch frequencies of non-hydrogen-bonded –OH group are observed at 3583 and 3672 $cm^{-1}$, respectively[64] (figure 4.2). These spectra have not been de-convoluted to elucidate the

exact nature of this free water[13,50,58,65]. Nonetheless, dilution of this sample to 50% with dried nitrobenzene decreases the intensity of the two IR peaks by 50%, further confirming that these peaks correspond to "free water".

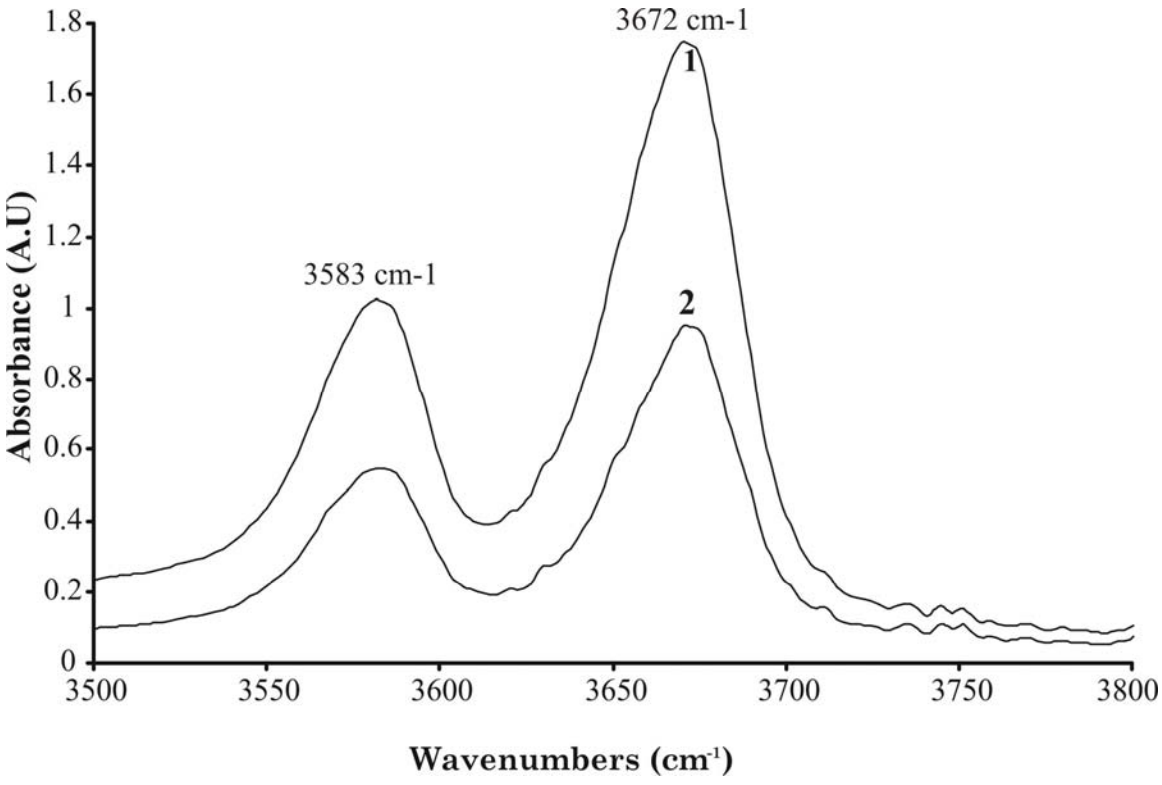


Figure 4.2: FTIR spectra of (1) wet nitrobenzene. (2) wet nitrobenzene diluted to 50% with dried nitrobenzene.

### 4.3.1 Cooling effect on IR spectra

Spectra of wet NB without (1,2) and with (3,4) $LiClO_4$ at room temperature and at 288K are shown in figure 4.3. The data suggests a minor decrease in free water content upon cooling (1 to 2). While this effect is not unambiguously detectable the decrease in free water due to the addition of $LiClO_4$ (1 to 3) is obvious. This result shows that $LiClO_4$ is capable of bonding significant amounts of free water in its solvation sphere. There is also noticeable thermal shift of the spectra on cooling.

### 4.3.2 Effect of anion identity on IR spectra

The spectrum of LiBr in wet NB (figure 4.4, spectrum 1) shows weak absorbance in the free water region. On dilution to 50% with wet nitrobenzene, spectrum (2) is observed. The increase in free water content is a factor of 10, indicating that the water ordering effect of the lithium has been disturbed by dilution. When solution of $LiClO_4$ in wet nitrobenzene (3) is diluted to 50% with wet nitrobenzene (4) the resulting absorbance in the free water region is indistinguishable from that of wet nitrobenzene (5). Separate to the dilution effects, it is clear from the significant differences between the $LiClO_4$ and LiBr spectra that the anion plays a major role in organization of water in the nitrobenzene phase.

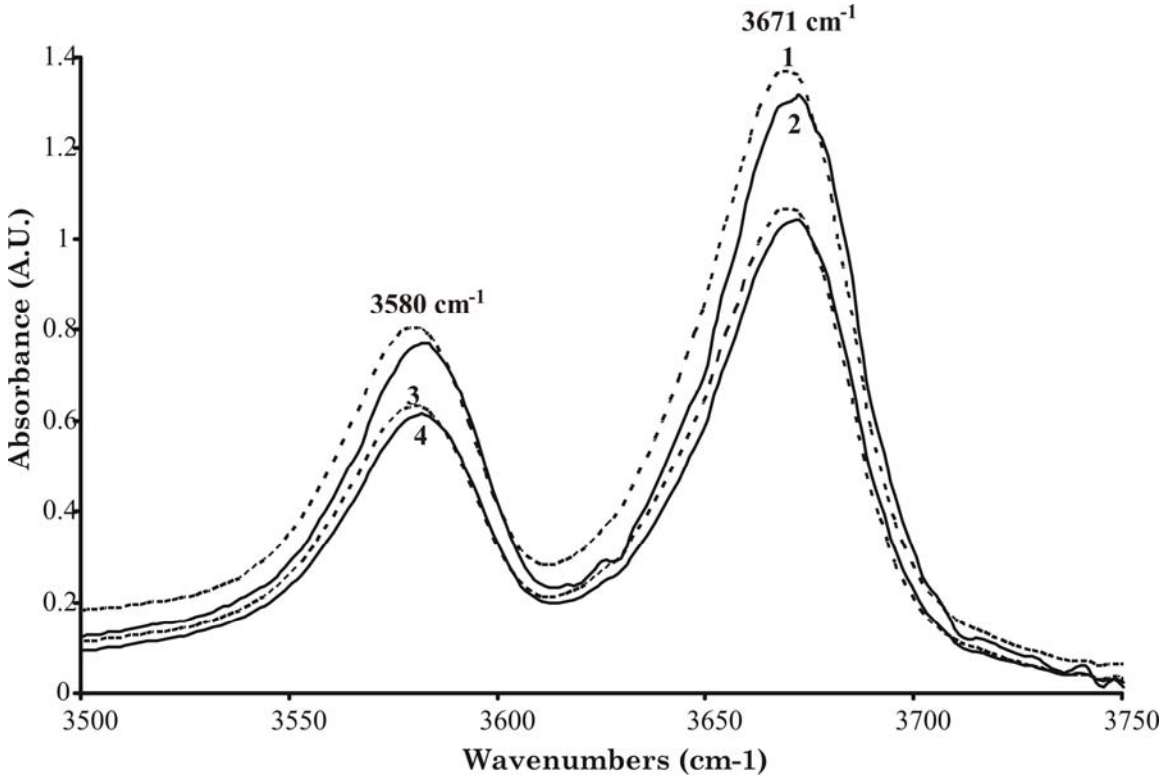


Figure 4.3: FTIR spectra of (1) wet NB at room temp. (2) Wet NB at $10^{o}$C. (3) $LiClO_4$/wet NB at room temp. and (4) $LiClO_4$/wet NB at $10^{0}$C.

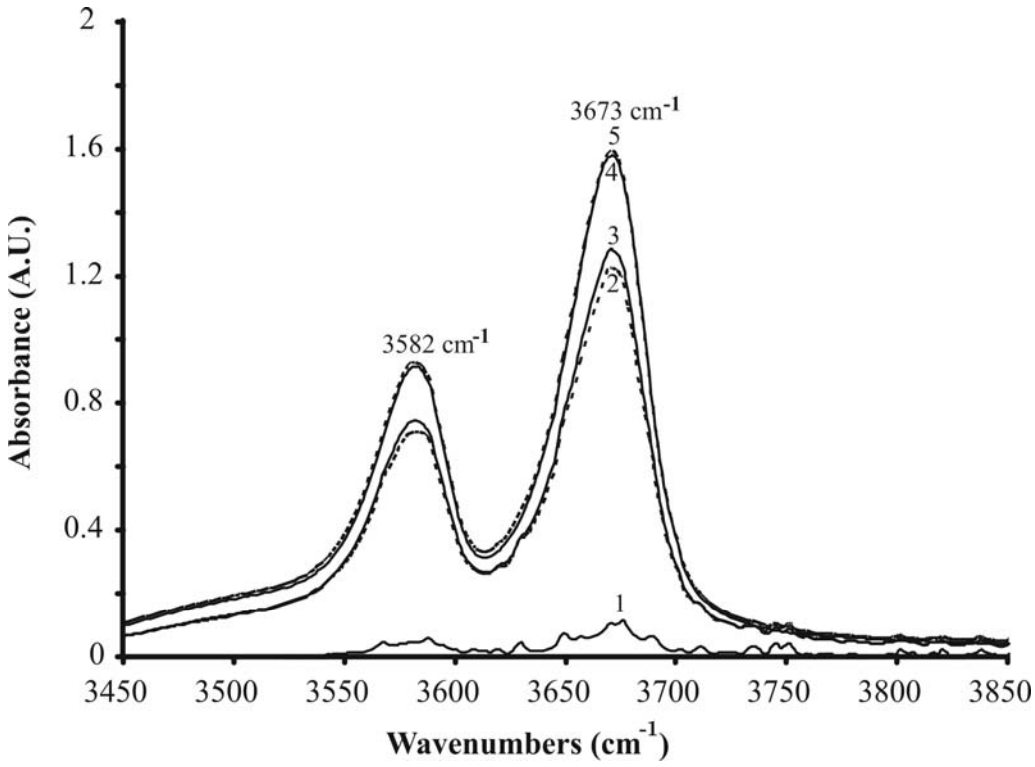


Figure 4.4: FTIR spectra of (1) LiBr/wet NB. (2) Diluted 50% with wet NB. (3) $LiClO_4$/wet NB. (4) Diluted to 50% with wet NB. and (5) Wet NB.

To further probe the importance of the anion in the ordering of water in NB, FTIR spectra were recorded of the three lithium salts LiBr, $LiClO_4$ and $LiHCB_{11}Me_{11}$ in wet NB (figure 4.5). The ability of the salt to order water, reducing free water content, decreases in that order.

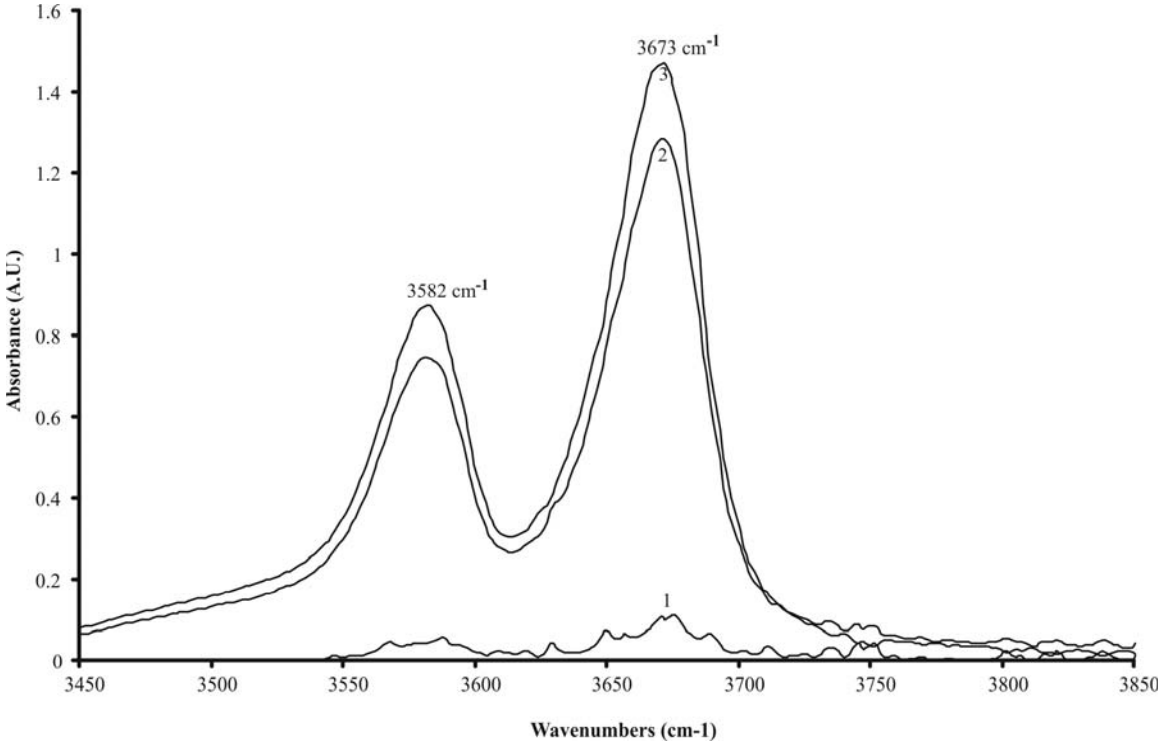


Figure 4.5: FTIR spectra of (1) LiBr/wet NB. (2) $LiClO_4$/wet NB and (3) $LiHCB_{11}Me_{11}$/wet NB.

In summary, the FTIR experiments have concluded that addition of lithium salt to wet nitrobenzene increases the occurance of hydrogen bonding between water molecules in the bulk nitrobenzene. The efficacy of 'LiX' on ordering of water increases with the hydrophobicity of the anion.

# CHAPTER V
# NEUTRON SCATTERING STUDY OF LITHIUM SALTS IN WATER-SATURATED NITROBENZENE

## 5.1 Introduction

Water in the organic phase gives rise to different IR stretches depending on the degree to which it is hydrogen bonded[61]. The effect of the anion on the "free" OH stretch at 3583 and 3672 $cm^{-1}$, respectively, has been studied by the FTIR. While FTIR can confirm that non-hydrogen-bonded species are 'tied up' by lithium, the structure of these clusters is still vague. The peaks in the above FTIR spectra are the symmetric and asymmetric stretch from non-hydrogen bonded OH. The structure of the bonded OH species cannot be studied by FTIR due to the large absorbance of the bulk solvent, nitrobenzene. It this chapter inelastic neutron scattering is used to elucidate the forms of water bonding in the nitrobenzene/water and nitrobenzene/water/lithium systems. The large inelastic scattering cross section of $H_2O$ vs. $D_2O$ is exploited by stirring deuterated nitrobenzene with $H_2O$, Scattering patterns arising from the various states of water are therefore not obscured by hydrogen atoms on the nitrobenzene as is the case when FTIR is used.

Comparison of the inelastic neutron scattering (INS) spectra for deuterated nitrobenzene which has been stirred with a) water b) saturated solution of $LiBr_{(aq)}$ is used to elucidate the affect of adding the lithium salt to the structure of the water clusters formed.

## 5.2 Experimental

### 5.2.1 Materials

Lithium bromide (≥99%, Aldrich) was used as received. D5-Nitrobenzene (99%, ACROS Organics) was redistilled under vacuum and dried before use by molecular sieves (4A, Sigma–Aldrich). All water used was de-ionized to 18 MΩ using a US-Filter Modulab water system (US Filter, Warrendale, PA).

### 5.2.2 Instrumentation

For the neutron scattering experiments, The Filter Difference Spectrometer (FDS) at the Manuel Lujan, Jr. Neutron Scattering Center (Los Alamos National Laboratory) was used. It measures the vibrational spectrum in neutron energy loss mode between 40 $cm^{-1}$ and 4000 $cm^{-1}$ with a white beam of neutrons. Determination of the neutron incident energy is by time-of-flight, whereas the final neutron energy is imposed by a set of beryllium filters between the sample and the detector banks. The instrument resolution varies from 4 to 7% across the energy range. This resolution can be further improved by the use of maximum entropy techniques during data analysis to 3-5%.

Protonated water ($H_2O$) and deuterated nitrobenzene ($C_6D_5NO_2$) were used to enhance the water signal while decreasing the scattering from nitrobenzene. Because the amount of water is small in comparison to the bulk nitrobenzene, the scattering

contribution from deuterated nitrobenzene remains significant. For this reason we collected a blank (pure nitrobenzene-$d_5$), as well as a spectrum for nitrobenzene-$d_5$ saturated with $H_2O$ and another nitrobenzene-$d_5$ sample stirred for 18 hours with $H_2O$ saturated with LiBr. The samples were placed in annular aluminum sample holders, 20 mm in diameter with an annular gap of 2 mm and a height of 100 mm. The aluminum wall thickness was 0.8 mm. All samples were quenched (from room temperature) in liquid nitrogen before being cooled rapidly to 12 K. When the temperature reached 12 K data collection started. Cooling was necessary because the vibrational modes broaden considerably with temperature. Because of the relatively high viscosity of the solutions and the rapid quenching, the material is likely amorphous and is probably representative of the disorder existing in the liquid state. All sample holders and sample volumes were identical.

## 5.3 Results

Figure 5.1 shows the neutron vibrational spectra for deuterated nitrobenzene saturated with $H_2O$ (thin line) and $LiBr_{(aq,\ saturated)}$ (thick line). Previous studies have proven LiBr to be particularly effective at ordering water in nitrobenzene hence the choice for this experiment. The internal modes of (deuterated) nitrobenzene were clearly observed above 500 $cm^{-1}$ in all the vibrational spectra. The high frequency part of the spectrum was not greatly affected by the presence of water and/or lithium bromide and was used to perform a (normalized for counting time and sample volume) blank subtraction. The low frequency part of the (blank-subtracted) spectra for nitrobenzene-

$d_5$+$H_2O$ and nitrobenzene-$d_5$+$H_2O$+LiBr are shown in Figure 5.1. There are some truly remarkable differences (and similarities) between the spectra.

The band that extends from 400 to 420 $cm^{-1}$ ("400 $cm^{-1}$ band") is one (or more) librational modes of water. For a water molecule in a general force field, there will be three librations, one for each axis of rotation, but these will be seen only if there is a restoring force present for each libration. There is the “rock”, which is motion in the plane of the water molecule; the “twist”, which is a rotation about the $C_2$ diad, and the “wag”, which is a rotation about the H-H axis, (typically) with increasing frequency[66]. In free water these librational modes are weak and appear as extremely broad, ill-defined bands in Raman and IR spectra, where they are at all detectable. In system in which water appears as a ligand to a metal cation, these librational modes become much more pronounced.[67] Notice that, unlike with optical spectroscopy, the librational modes are usually the strongest contribution to the vibrational spectrum of water.

Just as interesting is the disappearance of intensity in the vibrational spectrum at 175 and 220 $cm^{-1}$. These modes are usually attributed to hindered translations in ice and other forms of associated water molecules (clusters). According to Bertie and Whalley,[68] these modes are to be assigned to maxima in the density of vibrational states of water clusters owing to longitudinal acoustic and transverse optic vibrations, respectively. Their disappearance in the vibrational spectrum upon addition of LiBr is very likely indicative of a drastic rearrangement of water molecules in the system. Upon addition of LiBr to the system, some intensity appears as a shoulder on the high frequency side of the 260 $cm^{-1}$

peak (arrow in Figure 5.1) and is most likely associated with a Li-O stretching mode[69] - further proof of the association of water with $Li^+$.

The peaks at 260, and 350 $cm^{-1}$ are largely unaffected by the presence of LiBr in the system. However they are not present in the blank (pure nitrobenzene-$d_5$) and are undoubtedly associated with the presence of water in the system. The 260 $cm^{-1}$ mode may be associated with $H_2O$ molecules binding to nitrobenzene (N-O...H-O-H stretch).

The region between 280 and 320 $cm^{-1}$ (referred to here as the 300 $cm^{-1}$ band) is also characterized by a decrease in intensity upon addition of LiBr to the system. It is possibly another librational mode of water. If this is the case, it is tempting to associate the modes at 300, 350, and 400 $cm^{-1}$ to water librations. All three librational modes are present in the nitrobenzene-$d_5$ + $H_2O$ system. One mode is suppressed (rock) and one mode is enhanced (wag) when LiBr is added. The water twist at 350 $cm^{-1}$ seems unaffected. Its assignment as a librational mode is supported by its width, which is significantly larger than the sharp 260 $cm^{-1}$ mode.

In summary, the inelastic neutron scattering has added evidence to the FTIR results, which suggested that addition of lithium salt to the wet nitrobenzene phase increases the extent of hydrogen bonding between the water molecules. The technique has also confirmed the association of water around the lithium cation, as suggested by the earlier $^7Li$ and $^2H$ NMR experiments.

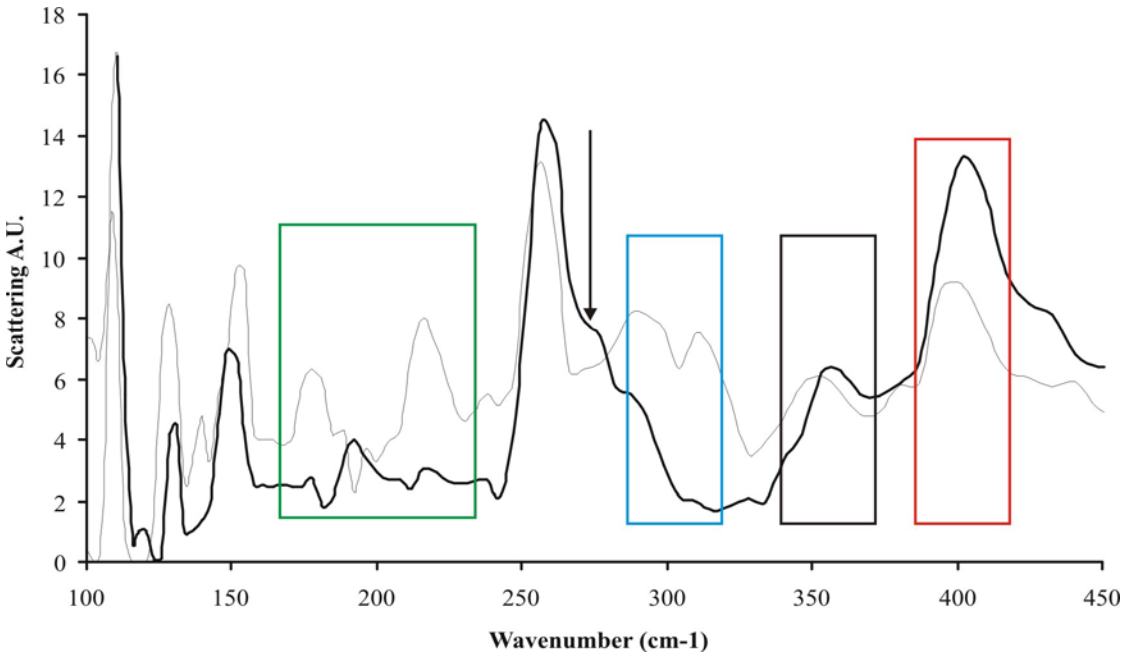


Figure 5.1: Neutron vibrational spectra of nitrobenzene-$d_5$ saturated with $H_2O$ (thin line) and nitrobenzene-$d_5$ saturated with $H_2O$+LiBr (thick line). The regions of the spectrum highlighted by boxes are discussed in the text.

# CHAPTER VI

# LITHIUM ION INCORPORATION IN GLASS

## 6.1 Introduction

Doping of materials with the lithium cation is technologically very significant. It is important in preparation of optical waveguides and other optoelectronic elements.[70-75] Lithium ion doping increases the refractive index of silicate, borosilicate, and phosphate glasses, resulting in the formation of a boundary at which the light is totally reflected. This interface is the key element for guided transmission of light in optical fibers and waveguides.

Lithium ion doping plays an important role in "anodic bonding".[76,77] Here lithium ion is introduced to the surface of a planar glass object that is to be joined with another glass object *without any other glue substance.* A high dc voltage (~1000 V) is applied while simultaneously heating the two objects (400 ºC) to be joined. Lithium ions from the donor surface migrate in the applied electric field to the acceptor surface. The resulting separation of charges causes formation of a strong electrostatic bond at the donor/acceptor boundary. This form of bonding is commonly employed in microelectromechanical systems technology where the use of any chemical adhesive could interfere with the intended use.

A third application involves the production of glass electrodes for pH and other cation determinations. Glass electrodes are among the oldest chemical sensors[78] for determination of activities of certain ions, such as hydrogen ion and alkali metal cations. Many different proprietary formulations of glass have been developed in order to control the chemical selectivity of these electrodes.[79] When an ordinary glass electrode is used for determination of pH in solutions containing high activity of alkali metallic cations, the so-called "sodium error" results. It is the result of the breakdown of the selectivity for protons that is caused by incorporation of alkali metal cations into glass. To suppress the response of the electrode to sodium ion relative to hydronium ion, special glasses containing a high concentration of lithium ion have been formulated.[80] However, processing of such glasses is more difficult and more expensive.

The processes by which the surface concentrations of certain desirable species are controllably changed fall into the broad category of *interface modification*. In the case of $Li^+$, the enhancement of interface concentration is accomplished by heating the object in molten Li salt,[81] by vacuum ion implantation, i.e., driving the accelerated $Li^+$ into the surface,[82,83] or by adding a thin layer of specially formulated material to the substrate, by thin-layer deposition techniques (e.g., sputtering) or thin-layer sol-gel deposition.[84,85] Each procedure has advantages and disadvantages related to the size and shape of the object to be treated, temperature compatibility, collateral damage of the matrix, economy of the process, and end use of the doped material.

In the course of investigations of solvation of lithium ion in a nitrobenzene/water system, it has been observed that $Li^+$ is rapidly transferred from "wet" nitrobenzene into

the hydrated, silica-containing walls of, for example, glass or quartz vessels. A hydrated layer that exists at the surface of these materials[11] attracts $Li^+$ from the organic phase. This transfer is driven by the high standard molar hydration Gibbs free energy of lithium ion ($= \Delta G^\circ_{hydr} = -481$ kJ.mol$^{-1}$ at 25°C).[16]

In this chapter, a simple procedure is described by which controlled lithium ion doping can be accomplished by exposing the acceptor surface to an organic solvent containing small amounts of water. It is likely that this principle can be extended to other ions, solvents, and surfaces to be treated. In the case of lithium ion and glass, the process can be described by simple ion-exchange equilibrium:

$$Li^+ (solution) + Na^+ (glass) = Li^+ (glass) + Na^+ (solution) \quad (1)$$

In other words, the lithium ion in solution is exchanged for sodium ion in glass. This is a dynamic equilibrium process described by the equilibrium constant $K_1$.

$$K_1 = a_{Li(g)}\, a_{Na(s)} / a_{Li(s)}\, a_{Na(g)} \quad (2)$$

Activity of incorporated $Li^+$ in glass therefore depends on $a_{Li(solution)}$, the activity of "free" (i.e., nonsolvated) $Li^+$ in solution because $Li^+$ solvated by organic solvent molecules cannot exchange into glass. If the solvent medium contains two or more types of solvent molecules, the solvation sphere is mixed and a solvatomeric equilibrium is established:[1]

$$Li^+(s) + xH_2O + yORG = Li^+(H_2O)_x(ORG)_y \quad (3)$$

The solvatomeric equilibrium constant, $K_s$ is defined as:

$$K_s = a_{Li(H2O)x(ORG)y} / a_{(H2O)}{}^{x}{}_{(ORG)}{}^{y} \quad (4)$$

$$\log a_{Li(glass)} = A + \log a_{Li(solution)} - x\log a_{(H2O)} \quad (5)$$

where the constant terms are:

$$A = pK_1 + pK_s + \log a_{Li(solution)} + \log a_{Na(glass)} - \log a_{Na(solution)} + y\log a_{(ORG)} \quad (6)$$

The term log $a_{Li\ (solution)}$ in eq 5 represents the total activity of lithium ion present in the organic phase. However, it is the "$x$ log $a_{H2O}$" term in eq 5 that dominates the $Li^+$ exchange. Lithium ion is strongly solvated by water, relative to all organic solvents. The standard free energy of transfer from nitrobenzene phase to water is $\Delta G^\circ_{W\text{-}NB}$ = -38 kJ.mol$^{-1}$ at 25 °C.[20] Therefore, the incorporation of $Li^+$ is driven by the total activity of solvated lithium ion present and by the *activity of water* in the organic phase. In other words, as the activity of water in organic phase *decreases,* the activity of $Li^+$ in glass *increases*. This phenomenon is analogous to the behavior of acidity (basicity) functions in mixed organic/aqueous media.[86]

In this chapter, we report on partitioning of $Li^+$ between organic solvent and glass, which can be used for controlled lithium ion doping. To determine the extent of $Li^+$ doping, we have used laser-induced breakdown spectroscopy (LIBS), a semiquantitative analytical technique that enables rapid, direct, and spatially and temporally resolved elemental analysis of solids or liquids. The LIBS experiment is initiated by directing a

high-power laser pulse onto the analyte; photon absorption by the sample creates localized plasma that efficiently vaporizes, atomizes, and excites the atoms. The emission spectrum from the plasma is composed of spectral lines characteristic of the elements present in the sample. Its predecessor is spark-source emission spectroscopy.[87] The major advantages of LIBS over other spectroscopic techniques are speed and simplicity of analysis, spatial resolution, and minimal sample preparation. Because of these advantages, LIBS has proven to be a widely applicable qualitative analysis method.[88] LIBS can be used for quantitative analysis provided that there is rigorous control of experimental factors.[89] LIBS is an efficient method for obtaining semi-quantitative, three-dimensional elemental profiles of samples. By rastering the laser pulse over the surface and recording the emission spectrum as a function of position, one can readily obtain the elemental distribution in the *xy* plane. Depth profiling can be accomplished by simply time gating repetitive laser pulses with spectral acquisition. Repeated pulsing of the laser results in ablation of the sample and exposure of material to the next pulse.[90]

Only a few applications of LIBS for the analysis of lithium have been published. Recently, Fabre and co-workers[91] used LIBS to determine the lithium content of geological samples. Synthetic glasses composed of lithium oxide in a silica matrix were used as standards in determining the lithium content of different geological materials. This approach afforded a detection limit of ~5 ppm.

## 6.2 Experimental Section

### 6.2.1 Materials.

Lithium bromide (99.95%, Strem Chemicals) was used as received. Nitrobenzene (NB; 99%, Acros Organics) was dried before use by molecular sieves (4A, Linde, Sigma-Aldrich). Microcoverslips (25 × 25 mm) were purchased from VWR Scientific (Catalog No. 48366 249). Polypropylene beakers, 50 mL in capacity, were obtained from VWR Scientific (Catalog No. 47751-694). All water used was deionized to 18 MΩ using a US-Filter Modulab water system (US Filter, Warrendale, PA).

### 6.2.2 Procedures.

Saturated solutions of LiBr in water were prepared by adding LiBr to deionized $H_2O$ until solid salt remained. For preparation of "wet" NB solution of LiBr, 5 mL of saturated aqueous solution was added to 20 mL of nitrobenzene. The two-phase mixture was magnetically stirred for 24 h. The phases were allowed to separate for 3 h, and after that, 5 mL each was transferred to several clean vials and then 3 mL of solution from each vial was transferred to 50-mL polypropylene beakers. The microcoverslips were then submerged in the LiBr/NB/$H_2O$ solution so that both sides of the coverslip were in contact with the solution. The beakers were then sealed with Parafilm, and each solution remained in contact with the coverslip for the appropriate contact time. Microcoverslips were then removed from solution and rinsed first by immersion for 10 s in 10 mL of acetone followed by rinsing for 5 s by a jet of acetone along each side of the coverslip. Acetone is miscible with nitrobenzene, permitting removal of solvated LiBr present on

the coverslip. Acetone does not, however, significantly dissolve LiBr. This reduces the risk of removing surface-sorbed lithium ions. Coverslips were allowed to air-dry for 1 h before commencement of analysis by LIBS. The equilibrium concentration of $Li^+$ in wet nitrobenzene solution was determined by atomic absorption spectroscopy to be $8.9 \times 10^{-5}$ M. Saturated concentration of water in pure nitrobenzene is 170 mM.[16]

### 6.2.3 Instrumentation

An Ocean Optics Inc. LIBS 2000+ instrument was used herein. This instrument enables the acquisition of high-resolution (0.1 nm) atomic emission spectrum over the range 200-980 nm. A Q-switched Nd:YAG laser (Ultra Big Sky Laser) high-energy laser pulse (50 mJ and duration of ~10 ns) is focused onto the sample by a 50-mm convex lens. A bundle of 600-m-diameter fibers collect emission from the plasma spark. A lens in front of the fiber bundle ensures that the plasma spark is sufficiently defocused that each fiber collects the same emission and eliminates spatial effects. Each fiber is connected to an individual grating monochromator that spatially disperses the emission onto a linear diode array detector. The data from each array is processed by the instrument and displayed. All spectra were collected with a 3.5-s delay and a 2-ms integration time. Spatial profiling of the elemental composition of the sample was achieved with an *x*-*y* translation stage. Each microcoverslip was securely taped to the translation stage of the instrument to avoid sample movement between laser shots.

Initially, many different combinations of laser energy and number of shots were attempted with clean, as-received micro cover glasses. This was performed to realize the technique that gives rise to the most reproducible LIBS response for known elements in

the glass. Consequently, all LIBS spectra were obtained from four laser shots, with the maximum energy setting of 10 (corresponding to 50 mJ/shot). Each displayed spectrum corresponds to the fourth laser shot taken. After completion of LIBS studies, the ablated areas of the glass were analyzed by profilometry. All profilometric traces were acquired using the Sloan Dektak 3 ST surface profilometer with Dektak 3 ST software. (Veeco Instruments).

## 6.3 Results

### 6.3.1 Laser Induced Breakdown Spectroscopy

Figure 6.1 shows two LIBS spectra, consisting of atomic emission intensity as a function of wavelength. Panel A shows the LIBS spectrum of a clean, untreated micro cover glass. The sodium content is clearly displayed by the two peaks (1 and 1') at ~589 (doublet, 3s - 3p, maximum arbitrary intensity $8.0 \times 10^4$) and ~819 nm (triplet, 3p - 3d, maximum arbitrary intensity $8.8 \times 10^3$). The absence of any significant Li peak supports the manufacturer's chemical composition data, which indicate that no lithium species are initially present in the micro cover glasses. Panel B shows the LIBS spectrum of a chemically identically micro cover glass exposed to a solution of LiBr in "wet" nitrobenzene for a total of 24 h. The Na peaks 1 and 1' have near-identical response to those in panel A. However, a significant Li transition peak (peak 2) is now observable at 671 nm (doublet, $1s^2 2s$ - $1s^2 2p$, maximum arbitrary intensity $3.6 \times 10^3$).

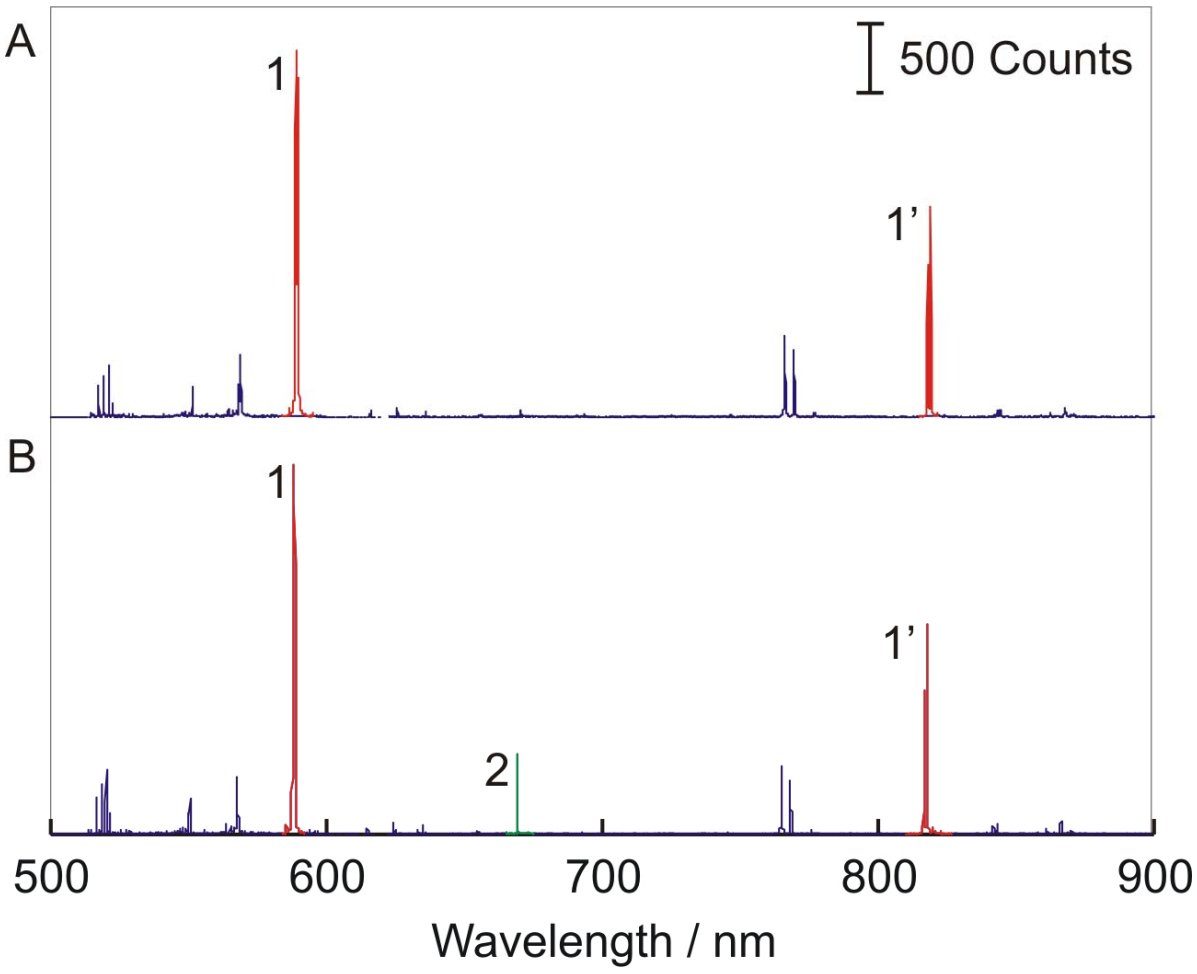


Figure 6.1 LIBS spectra of micro cover glasses: (A) clean, untreated cover glass; (B) cover glass exposed to "wet" nitrobenzene solution containing LiBr, for 24 h. Peaks 1, 1' correspond to $Na^+$ transitions at 589 and 819 nm. Peak 2 corresponds to a Li transition at 671 nm. [94]

Many different combinations of laser energy and number of laser shots fired were tried in an attempt to find a reproducible experiment. It was rationalized that after exposure to the LiBr in "wet" nitrobenzene solution, the ratio of Li to Na measured should be similar across one side of a single microcoverslip. As such, for each combination of laser energy and number of shots, the ratio of Li transition peak (671 nm) to Na transition peak (589 nm) was recorded, and after 10 LIBS measurements were made across the sample, the relative standard deviation of this ratio was calculated. This practice was repeated for each combination. The condition leading to the lowest standard deviation of results was to fire four laser shots at an energy of 50 mJ.

### 6.3.2 Profilometry

Profilometric studies were conducted on all samples in an attempt to explain the variance in the Li/Na ratio in single samples. Figure 6.2 shows four profilometric traces of holes created with these optimized conditions. It is clear that there are still significant variances in depth and shape of the ablated area, even when care is taken to ensure that the stylus follows the same path through each "hole" (through the greatest diameter of the hole). Thus, the variation in the mass of the ablated sample appears to be the main reason for the relatively large standard deviation. Figure 6.3 is a plot to show variation of Li content in a micro cover glass as a function of exposure time to LiBr in "wet" nitrobenzene. At each exposure time, 10 LIBS experiments were performed (4 laser shots at energy 50 mJ) and the ratio of Li (670 nm) to Na (588 nm) atomic emission responses was calculated for each experiment. The data points on this plot represent the average of the 10 ratio values.

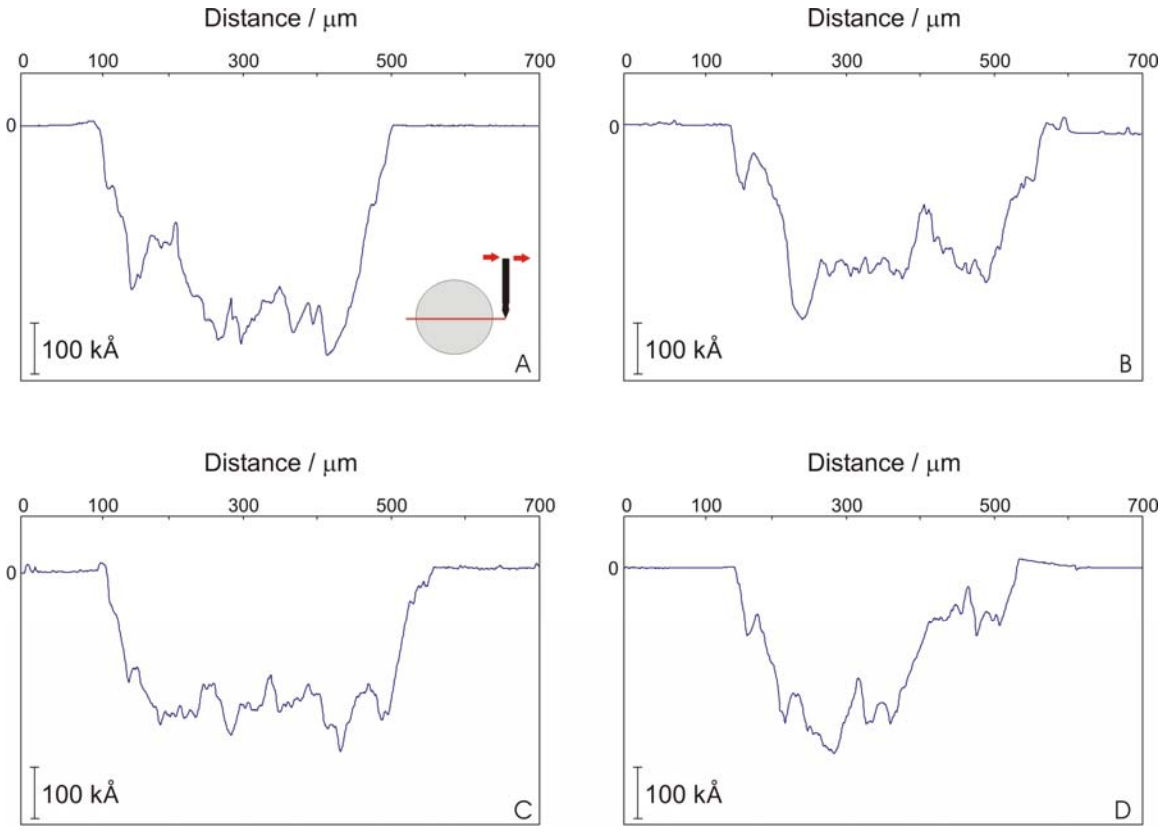


Figure 6.2: Profilometric traces of the craters created by the laser pulse in the coverslip. The trace was done always in the equatorial position (panel A). The variability in the diameter and in the depth of the craters accounts for the relatively large standard deviation of the signal.

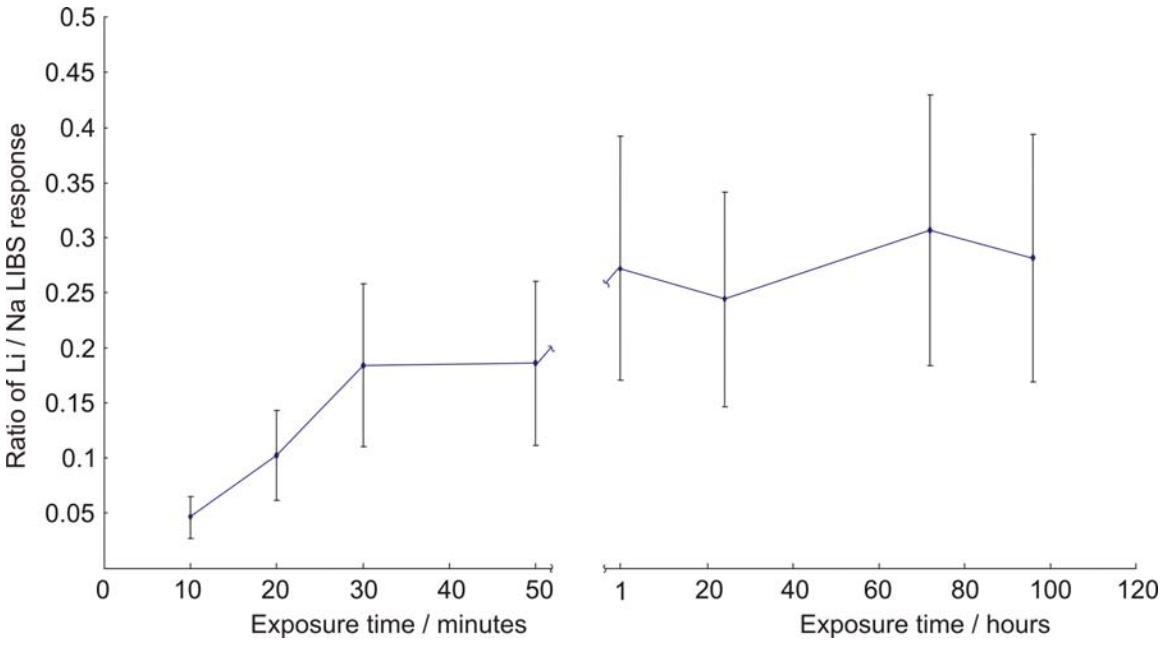


Figure 6.3: Dependence of the amount of $Li^+$ (relative to $Na^+$) as a function of exposure time.

### 6.3.3 Atomic Absorption

The depletion of $Li^+$ from the known volume of nitrobenzene mirrors its uptake by the glass. Standard size coverslips ($A$ = 6.25 $cm^2$) were immersed in 3.00 mL of 8.9 × $10^{-5}$ M LiBr contained in polypropylene beakers, for variable amounts of time. The concentration of remaining Li was determined by atomic absorption spectroscopy. The result shown in Figure 5.4 confirms the partitioning process.

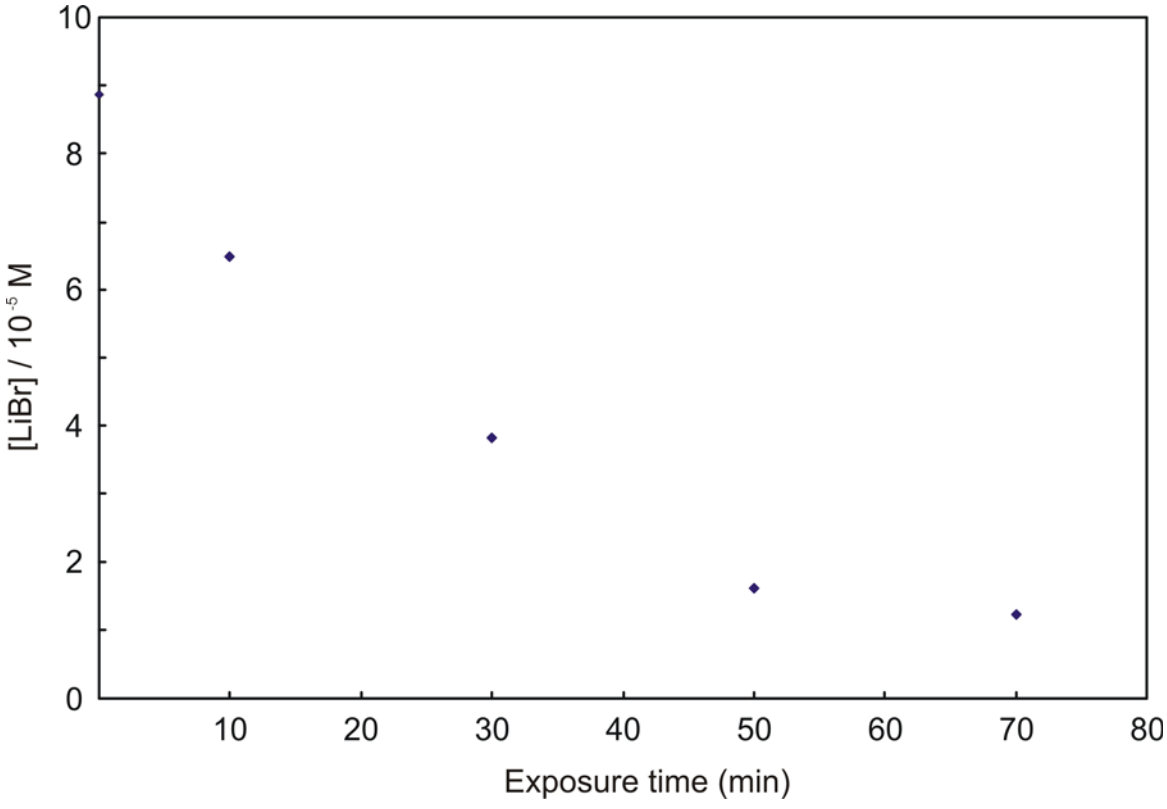


Figure 6.4: Depletion of $Li^+$ from 3.00 mL of 8.9 × $10^{-5}$ M LiBr by immersion of glass coverslips ($A$ = 6.25 $cm^2$) as a function of contact time.

# CHAPTER VII

# CONCLUSIONS

## 7.1 ITIES Studies

The original scope of this thesis work was to elucidate kinetics of ion transfer at the Interface of Two Immiscible Electrolyte Solutions (ITIES). The use of NMR to probe solvation is not new, but since NMR techniques require a homogeneous phase for measurement, observation of ions transferring across a liquid interface is usually not possible. In the work described in chapter I, we used molecular beads to suspend one phase inside the other, creating a paste wherein the two phases are in intimate contact. The kinetics of the equilibrium exchange of most ions between water and nitrobenzene, determined electrochemically is known to be very fast ($k \sim 10^{-1}$ cm $s^{-1}$). This has been confirmed by conducting an in situ 2D NMR experiment on the 'bead system', which consisted of $LiBr_{(aq)}$ contained within polystyrene beads and subsequently suspended in a bulk nitrobenzene phase. It appears that both very slow (on the scale of days) as well as very fast (milliseconds) processes are involved in the exchange of lithium ion between nitrobenzene and the aqueous phase.

Following the 2D NMR experiment, 1D $^{7}Li$ NMR experiments were conducted on the same bead experiment with hope of identifying solvation states of nitrobenzene that are involved in the transfer process. Unfortunately, heterogeneity of the sample led to broad resonances which obscured information on solvation states of lithium. Due to the

interference effects of the sephadex beads, the focus of the work shifted onto the study of the homogeneous 'wet nitrobenzene' phase, consisting of aqueous lithium salt dissolved in the nitrobenzene phase. In effect, this enables the study of the lithium species once it has already cross the ITIES into nitrobenzene, enabling us to answer the question: does the lithium retain its original solvation state in a metastable arrangement or exchange it with the bulk nitrobenzene?

### 7.2 Solvation of lithium in 'wet nitrobenzene' phase

Lithium ion profoundly affects the overall behavior of the NB/water system. Due to its high affinity for water $Li^+$ promotes transfer of water into NB. The coextraction of water into NB was determined by the Karl Fisher titration and the hydration numbers of a series of anions have been determined from spin–lattice relaxation times measured by $^1H$ NMR.[16] It has been found that six water molecules are associated with a lithium ion and two with a bromide ion. Since the two ions do not appear to form an ion pair there are at least eight moles of water bound by one mole of LiBr in ''wet'' nitrobenzene. With $Li^+$ concentration being determined as $1.43 \times 10^{-5}$ M and water concentration 60 mM there appears to be an excess of water to fully hydrate the LiBr salt.

The 1D $^7Li$ NMR results indicate that hydrated $Li^+$ in wet NB exists as a metastable species which slowly exchanges its solvation sphere through a series of equilibria involving multiple solvatomers over a period of days. The striking observation is the gradual merging of the two, initially well-resolved NMR resonances into one broad

peak that can be reversed by mechanical disruption (sonication). The slow changes attributable to solvation shell reorganization have not been observed or reported in $^{1}$H-NMR studies of the $Li^{+}$/NB/water system. It is not surprising because there is a much higher molar concentration of water in NB than of the lithium ion and the slow changes on the proton NMR signal originating from the hydration water of $Li^{+}$ are obscured by the excess, ‘‘free’’, uncoordinated water. It is interesting that where heating, microwave radiation and refluxing could not reverse the merging of the resonances, sonication could. However, if we consider that the slow forming species may be a large aggregate of water, approaching the μm range, such sonic energy would be deposited at the interface between the micro-sized water droplets and nitrobenzene, explaining how effective sonication is at disturbing the system.

Addition of $LiClO_4$ in place of LiBr gave immediate advantages in the study of solvation states. The concentration of $LiClO_4$ has a maximum of $9.52 \times 10^{-4}$M, as determined by atomic absorption spectroscopy. This is compared to $1.43 \times 10^{-5}$ M for lithium bromide. This significantly increased the signal to noise ratio of resulting $^{7}$Li NMR spectra, revealing resonances not visible in the LiBr studies and paving the way for kinetic studies of solvatomer evolution. Results suggests that at least three distinct but interconnected solvation states of lithium exist in the wet NB phase containing $Li^{+}$ and can be observed using $^{7}$Li as a NMR probe. A resonance at approximately 1.17 ppm is always observed in the system LiX/wet nitrobenzene. This resonance appears irrespective of anion type and is not affected by external perturbation of the equilibrium. This solvatomer has a similar chemical shift to $LiClO_4$ dissolved in dried nitrobenzene and as

such was deemed to be lithium solvated by a solvation sphere of majority nitrobenzene. This species is termed $Li_{NB}$.

An intermediate "metastable" solvatomer exists in the system $LiBr/H_2O$/nitrobenzene, and can be induced where less hydrophilic salts are used by cooling or on addition of small aliquots of water. The position of this peak is always approximately at 0.75 ppm. When considering that $LiClO_{4(aq)}$ and $LiClO_{4(NB)}$ produce resonances at ~ 0.4 ppm and 1.2 ppm respectively it is likely that this intermediate resonance results from lithium cation in a mixed solvation shell of water and nitrobenzene. This species is termed $Li_{NB/W}$.

A third resonance at ~ 0.4 ppm appears after addition of 5μL $LiClO_{4(aq,\ 1mM)}$ to $LiClO_4$/wet NB solution. An identical peak "grows" over a 12 hr period if the $LiClO_4$/wet NB solution is cooled in the presence of glass wall. These observations suggest that this third solvatomer is lithium solvated mostly by water, possibly nucleated on the glass surface since the presence of glass appears to be essential for observation of this peak. (the resonance is not present in experiments with Teflon lined tubes). This species is termed $Li_W$. On comparing the most upfield peak at 0.4 ppm to the spectrum of 20mM $LiClO_{4(aq)}$ (Fig. 2.6) the two spectra are very similar. This indicates that the amount of water solvating lithium is sufficient so that there is no appreciable effect of the bulk nitrobenzene on the $^7Li$ resonance shift.

In the initial $^{7}Li$ NMR experiments with LiBr/nitrobenzene/water, formation of multiple solvatomers of lithium in wet nitrobenzene was observed without a "supersaturation" step, by addition of water or by cooling. Lithium bromide is more hydrophilic than lithium perchlorate based on the relative positions of the anions in the Hoffmeister series. To fully understand the importance of the anion on the lithium environment in wet NB, we employed a lipophilic lithium salt, Lithium undecamethyl carba-closo-dodecaborate ($LiHCB_{11}Me_{11}$). It was dissolved in both dried nitrobenzene and wet nitrobenzene. The concentration of this salt in wet NB was restricted to 1mM to be of the same order of concentration as $LiClO_4$ in wet NB ($9.52 \times 10^{-4}$M). The resulting $^{7}Li^{+}$ spectrum showed a single resonance at 1.17 ppm which did not change upon cooling to 290K. This implies that with such a lipophilic anion, the lithium cation favors the predominantly nitrobenzene solvation shell. The type of the anion plays a key role in the solvatomers which can be observed in wet NB. If the lithium salt is highly hydrated (such as LiBr) multiple solvatomers can be observed by $^{7}Li$ NMR without perturbation. If the salt is moderately hydrated (such as $LiClO_4$) addition of aqueous phase or cooling will result in formation of solution which is supersaturated with water and thus observation of $LiX_{(NB/W)}$ and $LiX_{(W)}$ solvatomers occurs. If the salt is highly lipophilic (such as $LiHCB_{11}Me_{11}$) perturbation of LiX/wet NB solution fails to reveal multiple solvatomers.

The slow reorganization of the $Li^{+}$/nitrobenzene/water system can be represented by the scheme in figure 7.1 below. As seen in figure 2.9 the decay of metastable $Li_{(NB/W)}$ solvatomer is governed by first order kinetics. So is the increase of the $Li_{(NB)}$ solvatomer . However, the increase of the $Li_{(NB/W)}$ peak follows adsorption kinetics, corroborating the

effect of the glass wall. Apparently, one fraction of the $Li_{(NB/W)}$ loses nitrobenzene from its solvation shell and condenses on the hydrophilic glass wall while the other fraction loses water and reverts to the $Li_{(NB)}$ solvatomer. When the experiment is performed in the Teflon liner some $Li_{(NB/W)}$ reverts to $Li_{(NB)}$ but no $Li_{(W)}$ is observed. It is interesting to compare the experiments done in the presence of a glass wall and in it its absence. After approximately the same period of time (e.g. 11 hours) the $Li_{(NB/W)}$ solvatomer has completely disappeared in the case of the glass wall (Figure 2.8) while it remains in its 50% concentration in the Teflon tube (Figure 2.10). The glass wall clearly facilitates the decomposition of the $Li_{(NB/W)}$ solvatomer. The "wall effect" can be also considered from the point of view of interfacial electrostatics. Ions dissolved in the medium of high dielectric constant are repelled from the interface with a solid of lower dielectric constant, such as Teflon in our case. Therefore, the concentration of $Li_{(NB/W)}$ at the Teflon/nitrobenzene interface is much lower due to this repulsion and the break-up of the mixed solvation shell does not take place. A reverse effect takes place at the hydrophilic glass/NB interface which then actively participates in the destruction of the solvatomer.

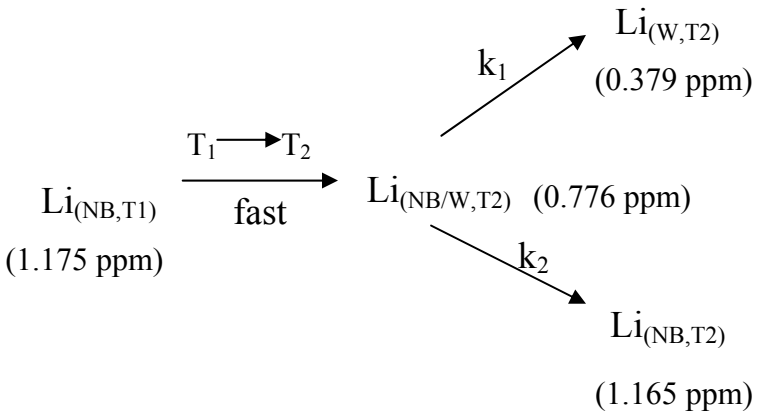


Figure 7.1: The slow reorganization of the $Li^+$/nitrobenzene/water system. $T_1$ indicates room temperature and $T_2$ indicates cooled solution.

### 7.3 Effect of lithium species on water bonding

As discussed above, the identity of the anion plays a key role in the solvatomers which can be observed in wet NB. If the lithium salt is highly hydrated (such as LiBr) multiple solvatomers can be observed by $^7$Li NMR without addition of water aliquots or cooling. If the salt is moderately hydrated (such as $LiClO_4$) addition of an aqueous phase or cooling will result in the formation of a solution which is supersaturated with water and thus the observation of $LiX_{(NB/W)}$ and $LiX_{(W)}$ solvatomers occurs. If the salt is highly lipophilic (such as $LiHCB_{11}Me_{11}$) cooling of the LiX/wet NB solution or addition of water fails to display multiple solvatomers. It was clear that the addition of lithium salt, and the identity of the anion, has a bearing on the solvatomers observed, but this effect could merely be due to differing amounts of water co-extracted into the nitrobenzene. To

assess whether the lithium species had a more substantial effect on the bonding within the solvatomers, the bonding between water molecules was probed.

This effect of lithium salts on the bonding of water in nitrobenzene was studied by FT-IR experiments, detecting the amount of free water in a $Li^+$/wet NB system. Systems where the $Li_{(NB/W)}$ or $Li_{(W)}$ states are difficult or impossible to form tend to have more free water in the NB phase.

Adding LiBr to wet Nitrobenzene lead to a system where the amount of free water is almost not detectable by FTIR. In contrast, when more lipophilic anions such as $ClO_4^-$ and $HCB_{11}Me_{11}^-$ were used, a detectable amount of free water remained dissolved in the nitrobenzene. This effect increases with the hydrophobicity of the anion.

From our NMR findings we expect that $Li^+$ in $LiHCB_{11}Me_{11}$/wet NB is only present as the $Li_{(NB)}$ solvatomer. In an ideal situation, the addition of ($LiHCB_{11}Me_{11}$) should therefore not affect at all the presence of free water as detected by IR. However, while IR data suggest that the water binding of $LiHCB_{11}Me_{11}$ is reduced in comparison to Li-salts with more hydrophilic anions, they still provide evidence of this binding effect. Also, it has been shown that for $LiClO_4$ cooling for extended amounts of time of wet Li NB solutions leads to the formation of hydrated $Li_{(W)}$ or $Li_{(W/NB)}$ species, which must have been formed from $Li^+_{(NB)}$ species. The NMR data suggest that ca. 30% of $Li_{(NB)}$ will be converted into hydrated $Li^+$ species (cf. for instances the peak intensities in Fig. 2.8). Observing the effect of temperature on a similar system using FT-IR exhibits only a

minor effect as to the release of free water (c.f. Figure 4.3). Hence, free water in NB appears to be not only affected by the hydration states of $Li^+$, other factors such as the identity of anion have to be of major influence as well. To summarize the FTIR findings, the lithium salts increase hydrogen bonding character of the water phase, with decreasing effect as the anion becomes more lipophilic. In the extreme, LiBr reduces free water content of the system effectively to zero versus a background of dried nitrobenzene.

Neutron vibration studies have added further evidence to the idea that addition of lithium bromide to water-saturated nitrobenzene results in a change in the hydrogen-bonding character of water. Overall, for the vibrational modes of 'free water', some of the modes are decreased and some increased by the addition of lithium bromide. Irrefutable, however, is the disappearance of intensity in the vibrational spectrum at 175 and 220 $cm^{-1}$ (figure 5.1), indicating a large change in the hydrogen bonding character on addition of LiBr. This supports the FTIR results. The FTIR and neutron scattering results jointly suggest that addition of lithium salts to 'wet nitrobenzene' has an affect on the state of water. The more hydrophilic the anion, the greater the hydrogen bonding of the water around the salt explaining the increasing number of solvation states observable in the $^7Li$ NMR spectra as we move from $LiHCB_{11}Me_{11}$, to $LiClO_4$ to LiBr.

### 7.4 Role of Lithium in solvatomer formation

It has been proven that lithium salts, dependant on the identity of the anion, are capable of promoting hydrogen bonding in water dissolved in nitrobenzene. This does

not, however, prove our initial thoughts that lithium salts can promote formation of large water aggregates in the nitrobenzene. The result only has implications of the nature of water bonding. While it is clear that lithium salts increase the number of observable solvation states in wet nitrobenzene, it was difficult to know if these states were actually created by addition of lithium. The drawback of the $^{7}$Li NMR experiments was that the presence of lithium as a reporter ion is essential. As such, it was impossible to determine the state of water dissolved in the nitrobenzene without a lithium salt present. The use of deuterium as a reporter ion provided further evidence that multiple solvatomers can be observed in the Li/nitrobenzene/water system studied. This technique has provided a method by which to compare water organization in nitrobenzene with and without the presence of lithium species.

Without cooling or addition of water aliquots, only one peak was observable in the $^{2}$H NMR spectra. This peak appeared at ~-2 ppm versus a pure $D_2O$ sample that was calibrated to 0ppm. This peak shifted downfield towards zero on cooling and addition of LiX salts. We can conclude from this that $Li^+$ promotes the formation of aggregate water solvatomers such as $Li_{NB/W}$ and $Li_W$. As the number of these solvatomers increases, the average NMR shift observed becomes more similar in character to the calibrant, $D_2O$. However, addition of a 5μL aliquot of $D_2O$ to nitrobenzene without LiX salts revealed three solvatomers analogous to those from the $^{7}$Li experiments. This means that even though $Li^+$ promotes the formation of multiple solvation states, these states exist to some degree in the absence of lithium, especially if the water content is increased to the level of precipitation.

Kinetic studies have supported previous reports that perturbation of the system by addition of water aliquot leads to three solvatomers that undergo a slow dynamic exchange over 180 minutes following addition of water. The main feature of these kinetics appears to be the appearance and subsequent decomposition of a metastable solvatomer consisting of $Li^+$ solvated by a mixture of water and nitrobenzene. As this species decomposes, the resulting "free" water appears to be incorporated in the species we have termed $Li_{NB}$ and $Li_W$. These are solvatomers comprising a majority of nitrobenzene and water, respectively.

Diffusion ordered spectroscopy has elucidated diffusion coefficients and hydrodynamic radii for water dissolved in nitrobenzene. Addition of lithium to the system has a negligible effect on both. It was noted that the hydrodynamic radius of water species in nitrobenzene $Li_{(NB)}$ is somewhat smaller than that of bulk water. It was observed that the solvatomer $Li_{(NB/W)}$ has a similar hydrodynamic radius to that of bulk water. The major conclusion from the DOSY studies is that while addition of lithium to wet nitrobenzene may result in increased hydrogen bonding and promotion of aggregate formation, it does not have a significant effect on the size of water aggregates, but instead affects only the bonding of water.

### 7.5 Lithium incorporation into glass

It is not generally appreciated that any oxide surface that is exposed to "wet" organic phase will rapidly adsorb lithium and possibly other ions. As long as there is the

aqueous phase containing a large molar excess of $Li^+$, the equilibrium at the liquid/liquid interface is not likely to be affected. Our discovery that the $Li^+$ uptake by the glass walls of the vessels used in the experiments can be used for doping purposes was purely serendipitous. However, it is obvious that nitrobenzene can be replaced by other, less toxic and more environmentally friendly organic solvents, as long as they satisfy the requirement of large negative Gibbs free energy of transfer to water. Similarly, other ions with large standard free energy of hydration, such as $Mg^{2+}$, $Ca^{2+}$, or $Al^{3+}$, can be incorporated into a hydrated layer of the solid from a suitable mixed aqueous/organic solvent. The available databases of solvation energies and standard Gibbs free energies of transfer[92,93] can aid the design of appropriate experimental doping conditions. Laser-induced breakdown spectroscopy is an efficient and effective tool for monitoring such experiments.

The main feature that distinguishes the mixed solvent ion doping process from other forms of surface modification by ions is the mild condition under which the ions are introduced to the surface of the solid material. There is no collateral damage to the matrix of the recipient material, as would be experienced in, for example, ion implantation. The treatment is done at room temperature and involves a relatively short exposure of the surface to organic solvent containing dopant ion (here lithium ion) salt. This is important in applications where elevated temperature could cause delamination due to mismatched thermal expansion coefficients of, for example, laminated and composite materials. The length of the exposure varies from solid to solid and depends also on the depth of the doped zone. The exposure is typically in tens of minutes. It is controlled primarily by the mole fraction of water in the organic solvent.

Besides the mild treatment conditions, another advantage is that it is possible to treat geometrically convoluted surfaces and localized areas. That is certainly not the case for other doping methods such as ion implantation or spin-on sol-gel process. Finally, the process is very economical because the source chemicals are inexpensive, can be recycled, and no expensive equipment is necessary. Investigations of other solvent/ion/interface systems are desirable.

## 7.6 Summary of findings

There exist three major water environments when water is dissolved in nitrobenzene. $^{2}H$ NMR proves that these solvatomers exist irrespective of whether lithium salt is added to the system. $^{7}Li$ NMR experiments suggest that the first solvatomer is majority nitrobenzene, the second a mixed solvation shell consisting of some ratio of nitrobenzene and water and the third solvatomer is large water aggregate of immobilized water on glass surface. The mixed solvation state is short lived and can be promoted by addition of water aliquot of by supersaturating the system upon cooling. This is a high energy state and will decay either back into the homogenous bulk NB state or to the surface of the glass wall, depending on if there is a glass surface present. In the $^{7}Li$ NMR experiments, the hydrophobicity of the salt, determined by the anion, effects the relative intensity of the three $^{7}Li$ resonances. This makes sense, since the hydrophobicity dictates which of these three solvation states is preferred by the salt.

Addition of lithium serves to promote hydrogen bonding in the majority nitrobenzene solvatomer, as confirmed by FTIR and neutron diffraction studies. There is no evidence that it has effect on the size of the mixed solvatomer or the water aggregate immobilized on the glass surface. A reasonable hypothesis is that lithium exchanges between the water species which are formed independent of lithium involvement. The system can be summarized as follows:

Below critical water concentration (~200mM) nitrobenzene/water is a homogeneous distribution of water molecules in nitrobenzene. Addition of lithium salt to such a system has two main affects. First, the lithium promotes hydrogen bonding between the dissolved water molecules, as confirmed by FTIR and neutron scattering. Second, the hydrogen bonded water may precipitate causing microheterogeneity of the system, leading to a second resonance observed in both the $^{2}H$ and $^{7}Li$ NMR spectra ($Li_{NB/W}$). In the presence of glass, a third solvation state can nucleate at the glass surface, this solvation state has character even closer to that of bulk water ($Li_{W}$). These two supplementary solvation states can be artificially induced by either adding aliquots of water or cooling.

# CHAPTER VIII

# FUTURE WORK

Through use of $^{2}H$, $^{7}Li$ NMR, FTIR, Atomic Absorption and Neutron Scattering, we have added to the information known about the solvation environments of salts in a mixed water/organic system. It is likely that some or all of these techniques used could add useful information on other relevant mixed solvent system such Room Temperature Ionic Liquids (RTILs) a field of study which is attracting considerable interest, not least for use in batteries.[95-97]

Room-temperature ionic liquids are rapidly increasing in popularity as a topic of research. This is due to their unique solvent properties, for example low volatility, high chemical, thermal, and electrochemical stability, high ionic conductivity, and hydrophobicity.[98] These properties make them very plausible electrolytes for use in electrochemistry applications like electrodeposition, light-emitting electrochemical cells, electrochemical capacitors, fuel cells, and batteries.[98] Lithium-ion batteries using such electrolytes have excellent performance at temperatures as low as 313 K.[99] The use of RTILs as electrolytes for supercapacitors has also been demonstrated.[99] Mixtures of room temperature ionic liquids with lithium salts, LiX are predicted to improve the performance of supercapacitor electrolytes.[99] Although RTILs are purely ionic, the anion and cation of the liquid are not typically electroactive in the lithium battery. As such, addition of lithium salt to the RTIL is required if it is to be used as a medium for the battery.

One of the issues surrounding this addition of lithium salt is a lack of understanding of solvation environments with the liquid.[40] The solvation of lithium in the system, both by the ionic liquid itself and dissolved water has implications on the conduction mechanism for the lithium species. Experiments must therefore be designed to probe the solvation environments of lithium in mixed systems of RTILs and water. The structure of water in RTILs has been probed by observing OH stretches in FTIR.[40] There is no structural information available on the mixed system LiX/RTIL/water. Future work will involve conducting $^{2}H$ and $^{7}Li$ NMR studies on such a system to assess the solvation environment of lithium. The potential for these experiments are extensive due to the number of RTILs available by varying anion and cation of the liquid itself. This may lead to experiments where the solvation environment of lithium is observed as a function of changing water content of the ionic liquid. Customizing the ionic liquid leads to a large range of hydrophobicity of the liquid.

# REFERENCES


[1] Samec, Z., *Pure Appl. Chem.*, 2004, 76, 2147

[2] Kakiuchi, T., Senda, M., *Bull. Chem. Soc. Jpn., 1984,* 57, 1801

[3] Mareček, V., Samec, Z., *Anal. Lett.,* 1981 14(B15), 1241

[4] Koryta, J., *Electrochim. Acta*, 1988, 33, 189

[5] Reymond, F., Fermin, D., Jin, H., Girault, H. H., Electrochim. Acta, 2000, 45, 2647

[6] Kontturi, K., Manzanares, J. A., Murtomaeki, L., Schiffrin, D. J., *J. Phys. Chem. B*, 1997, 101, 10 801

[7] Scholz, F., Gulaboski, R., Caban, K., *Electrochem. Commun*., 2003, 5, 1388

[8] Kakiuchi, T., Teranishi, Y., *Electrochem. Commun*., 2001, 3, 168

[9] Samec, Z., *Electrochim. Acta*, 1998, 44, 85

[10] Samec, Z., Kharkats, Y., Gurevich, Y. Y., *J. Electroanal. Chem*., 1986, 204, 257

[11] Vanysek, P., Lecture Notes in Chemistry, Springer–Verlag, New York, 1985, vol. 39.

[12] Scatena, L. F., Brown. M. G., Richmond, G. L., *Science*, 2001, 292, 908

[13] Richmond, G. L., *Annu. Rev. Phys. Chem*., 2001, 52, 357

[14] Watry, M. R., Brown, M. G., Richmond, G. L., *Appl. Spectrosc*., 2001, 55, 321A

[15] Girault, H. H., Schiffrin, D. J., *Electrochim. Acta*, 1986, 31, 1341

[16] Osakai, T., Hoshino, M., Izumi, M., Kawakami, M., Akasaka, K., *J. Phys. Chem. B,* 2000, 104, 12 021

[17] Osakai, T., Ogawa, H., Ozeki, T., Girault, H. H., *J. Phys. Chem. B,* 2003, 107, 9829

[18] Osakai, T., Ogata, A., Ebina, K., *J. Phys. Chem. B*, 1997, 101, 8341

[19] Osakai, T., Tokura, A., Ogawa, H., Hotta, H., Kawakami, M., Akasaka, K., *Anal. Sci,* 2003, 19, 1375

[20] Osakai, T., Ebina, K., *J. Phys. Chem. B*, 1998, 102, 5691

[21] Mareček, V., Samec, Z., *Anal. Chim. Acta,* 1983, 151, 265

[22] Samec, Z., Mareček, V., Weber, J., Homolka, D., *J. Electroanal. Chem.*, 1981 126, 105

[23] Geblewicz, G., Schiffrin, D. J., *J. Electroanal. Chem.,* 1988, 244, 27

[24] Samec, Z., *Chem. Rev*., 1988, 88, 617

[25] Girault, H. H., Schiffrin, D. J., In *Electroanalytical Chemistry*, Vol. 15, A. J. Bard (Ed.), p. 1, Marcel Dekker, New York (1989).

[26] Samec, Z., Kakiuchi, T., In *Advances in Electrochemistry and Electrochemical Science*, Vol. 4, $_{21}$H. Gerischer and C. W. Tobias (Eds.), p. 297, VCH, Weinheim (1995).

[27] Volkov, A. G., Deamer, D. W., (Eds.). *Liquid–Liquid Interfaces: Theory and Methods*, CRC Press, Boca Raton (1996).

[28] Testa, B., Kier, L. B., Carrupt, P. A., *Med. Res. Rev*., 1997, 17, 30

[29] Smith, D. A., Jones, B. C., Walker, D. K., Med. *Res. Rev.* 1996, 16, 243

[30] Nernst, W., *Z. Phys. Chem., 1892,* 9, 137

[31] Gavach, C., Henry, F., *J. Electroanal. Chem., 1974,* 54, 361

[32] Shao, Y., Girault, H. H., *J. Electroanal. Chem., 1990,* 282, 59

[33] Kakutani, T., Osakai, T., Senda, M., *Bull. Chem. Soc. Jpn.,* 1983, 56, 991

[34] Samec, Z., Mareček,V., Weber, J., *J. Electroanal. Chem.,* 1979, 100, 841

[35] Samec, Z.,*J. Electroanal. Chem.,* 1980, 111, 211

[36] Samec, Z., Mareček, V., Homolka, D., *J. Electroanal. Chem.* 1981, 126, 121

[37] Gavach, C., Seta, P., Henry, F., *Bioelectrochem. Bioenerg* 1974, 1, 329

[38] Grandjean, J., *Annu. Rep. NMR Spectrosc.*, 1998, 35, 217

[39] Tong, Y,. Oldfield, E., Wieckowski, A., *Anal. Chem.*, 1998, 70, 518A

[40] T. Köddermann, F. Schulte, M. Huelsekopf and R. Ludwig, *Angew. Chem., Int. Ed.* 42 (2003), pp. 4908–4909.

[41] Abraham, M. H., Liszi, J., Meszaros, L. J Chem. Phys. 1979, 70, 2491.

[42] Abraham, M. H., Liszi, J. J Inorg. Nucl. Chem. 1981, 43, 143.

[43] Osakai, T., Ebina, K., J. Electroanal. Chem. 1996, 412, 1.

[44] Ito, K., Iwamoto, E., Yamamoto, Y. Bull. Chem. Soc. Jpn. 1983, 56, 2290.

[45] Stokes, G. G., Mathematocal and Physical Papers, Cambridge University press, 1901, 3, 55.

[46] Buch, V., Devlin, J. P. J. Chem. Phys. 1999, 110, 3437.

[47] Wojcik, M. J., Buch, V., Devlin, J. P., J. Chem. Phys. 1993, 99, 2332.

[48] Buch, V., Devlin, J. P., J. Chem. Phys. 1991, 94, 4091.

[49] Zwier, T. S., Science, 2004, 304, 1119.

[50] Max, J. J., de Blois, S., Veilleux, A., Chapados, C., Can. J. Chem., 2001, 79, 13.

[51] Miazaki, M., Fujii, A., Ebata, T.,Mikami, N., Science, 2004, 304, 1134.

[52] Gragson, D.E., Richmond, G. L., J. Chem. Phys., 1997, 107, 9687.

[53] Scatena, L. F., Richmond, G. L., Science, 2001, 292, 908.

[54] Du, Q., Superfine, R., Freysz, E., Shen, Y. R., Phys, Rev. Lett., 1993, 70, 2313.

[55] Linse, P. J., J. Chem. Phys., 1987, 86, 4177.

[56] Brown, M. G., Walker, D.S, Richmond, G. L., J. Phys. Chem., 2002.

[57] Venables, D. S., Schmuttenmaer, C. A., J. Chem. Phys., 1998, 108, 12, 4935.

[58] Takamuka, T., Tabata, M., Yamaguchi, A., Nishimoto, J., J. Phys. Chem. B., 1998, 102, 8880.

[59] Bonner, O. D., Choi, Y. S., J. Phys. Chem, 1974, 78, 17, 1723.

[60] Bonner, O. D., Choi, Y. S., J. Phys. Chem, 1974, 78, 17, 1727.

[61] Kodderman, T., Wertz, C., Neintz, A., Ludwig, R., Angew. Chem. Int. Ed., 2006, 45, 3697.

[62] Cammarata, L., Kazarian, S. G., Salter, P. A., Welton, T., Phys. Chem. Chem. Phys., 2001, 3, 5192.

[63] Silverstein, R. M., Webster, F. X., Spectrometric Identification of Organic Compounds, sixth ed., Wiley & Sons, New York, 1998.

[64] Koddermann, T., Schulte, F., Huelsekopf. M., Ludwig, R., Angew. Chem. Int. Ed., 2003, 42, 4908.

[65] Leich, M. A., Richmond, G. L., Faraday Trans., 2005, 129, 1

[66] D.Eisenberg and W. Kauzmann, "The Structure and Properties of Water," (Oxford University Press, Oxford, 1969), Sections 3.5 and 4.7.

[67] G. Socrates, "Infrared and Raman Characteristic Group Frequencies - Tables and Charts," (John Wiley and Sons, Ltd, Chichester, 2001), 3rd Edition.

[68] Bertie, J.E., and Whalley, E., J.Chem.Phys., 1967, 46, 1271

[69] Rudolph, W., Brooker, M. H., Pye, C. C. J.Phys.Chem., 1995, 99, 3793

[70] Hazart, J., Vincent, M. French Patent 2831277.

[71] Fujisawa, T.; Hakamata, K.; Harada, T.; Ito, M.; Hayashi, T.; Ichikawa, T. Japanese Patent 2003172840.

[72] Houde-Walter, S. N. *Proc. SPIE Int. Soc. Opt. Eng.* 1988, *935*, 2

[73] Wong, S. F., Pun, E. Y. B., Chung, P. S. *IEEE Photonics Technol. Lett*. 2002, *14*, 80

[74] Podvyaznyi, A. A., Svistunov, D. V. *Technol. Phys. Lett*. 2003, *29*, 456

[75] McCov, M. A.; Zimmermann, J. W. U.S. Patent 20030196455.

[76] Hirschfeld, D. A., Schubert, W. K., Watson, C. S. U.S. Patent 20030092243.

[77] Watson, C. S., Hirschfeld, D. A., Schubert, W. K. *Ceram. Eng. Sci. Proc.* 2002, *23*, 877

[78] Cremer, M. *Z. Biol.* 1906, *47*, 562

[79] Morf, W. E. *The Principles of Ion-Selective Electrodes and of Membrane Transport.*; Elsevier: New York, 1981.

[80] Bach, H., Baucke, F. G. K. *Phys. Chem. Glasses* 1974, *15*, 123

[81] McCov, M. A., Zimmermann, J. W. U.S. Patent 20030196455.

[82] Job, R., Werner, M., Denisenko, A., Zaitsev, A. M., Fahrner, W. R. *Diamond Relat. Mater.* 1996, *5*, 757

[83] Kajihara, S. A., Antonelli, A., Bernholc, J., Car, R. *Phys. Rev. Lett.* 1990, *15*, 2010

[84] Minami, T., Hayashi, A., Tatsumisago, M. *Solid State Ionics* 2000, *136*, 1015

[85] Tatsumi, K., Hibino, M., Kudo, T. *Solid State Ionics* 1997, *96*, 35

[86] Reichardt, C. *Solvents and Solvent Effects in Organic Chemistry*; VCH Publishers: Weinheim, 1990.

[87] Boumans, P. W. J. M. In *Analytical Emission Spectroscopy*; Grove, E. L., Ed.; Marcel Dekker: New York, 1972; Vol.1, Part 1.

[88] Lee, W. B.,Wu, J., Lee, Y. I., Sneddon, J. *Appl. Spectrosc. Rev.* 2004, *39*, 27

[89] Tognoni, E.; Palleschi, V.; Corsi, M.; Cristoforetti, G. *Spectrochim. Act* 2002, *57*, 1115

[90] Papazoglou, D. G., Papadakis, V., Anglos, D. *J. Anal. At. Spectrom.* 2004, *19*, 483

[91] Fabre, C., Boiron, M. C., Dubessy, J., Chabiron, A., Charoy, B., Crespo, T. M. *Geochim. Cosmochim. Acta* 2002 *66* (8), 1401

[92] Marcus, Y. *Rev. Anal. Chem.* 1980, 53(5), 421.

[93] Marcus, Y. *Ion Solvation.*; Wiley: Chichester, U.K., 1985.

[94] NIST Atomic Spectra Database, www.physics.nist.gov/cgi.

[95] Song, C. E., Shim, W. H., Roh, E. J., Lees, S. G., Choi, J. H., *Chem. Commun.*, 2001, 1122

[96] Gordon, C. M., Hilgers, C., Muldoon, M. J., Dunkin, I. R., *Chem. Commun*., 2001, 1186

[97] Chen, Z., Dahn, J. R., *Electrochem. Solid-State Lett*., 2003, 6, A221

[98] Blanchard, L. A., Gu, Z., Brennecke, J. F., *J. Phys. Chem. B*., 2001, 105, 2437

[99] Hammami, A., Ramond, N., Armand, M., *Nature (London)*, 2003, 242, 635